*J Appl Physiol* 100: 1278–1286, 2006.
First published December 22, 2005; doi:10.1152/japplphysiol.01206.2005.

TRANSLATIONAL PHYSIOLOGY

# Automated drug delivery system to control systemic arterial pressure, cardiac output, and left heart filling pressure in acute decompensated heart failure

**Kazunori Uemura,[1] Atsunori Kamiya,[1] Ichiro Hidaka,[1] Toru Kawada,[1] Shuji Shimizu,[1] Toshiaki Shishido,[1] Makoto Yoshizawa,[2] Masaru Sugimachi,[1] and Kenji Sunagawa[3]**

[1]*Department of Cardiovascular Dynamics, National Cardiovascular Center Research Institute, Suita;* [2]*Research Division on Advanced Information Technology, Information Synergy Center, Tohoku University, Sendai;* [3]*Department of Cardiovascular Medicine, Kyushu University Graduate School of Medical Science, Fukuoka, Japan*

Submitted 22 September 2005; accepted in final form 17 December 2005

**Uemura, Kazunori, Atsunori Kamiya, Ichiro Hidaka, Toru Kawada, Shuji Shimizu, Toshiaki Shishido, Makoto Yoshizawa, Masaru Sugimachi, and Kenji Sunagawa.** Automated drug delivery system to control systemic arterial pressure, cardiac output, and left heart filling pressure in acute decompensated heart failure. *J Appl Physiol* 100: 1278–1286, 2006. First published December 22, 2005; doi:10.1152/japplphysiol.01206.2005.—Pharmacological support with inotropes and vasodilators to control decompensated hemodynamics requires strict monitoring of patient condition and frequent adjustments of drug infusion rates, which is difficult and time-consuming, especially in hemodynamically unstable patients. To overcome this difficulty, we have developed a novel automated drug delivery system for simultaneous control of systemic arterial pressure (AP), cardiac output (CO), and left atrial pressure (Pla). Previous systems attempted to directly control AP and CO by estimating their responses to drug infusions. This approach is inapplicable because of the difficulties to estimate simultaneous AP, CO, and Pla responses to the infusion of multiple drugs. The circulatory equilibrium framework developed previously (Uemura K, Sugimachi M, Kawada T, Kamiya A, Jin Y, Kashihara K, and Sunagawa K. *Am J Physiol Heart Circ Physiol* 286: H2376–H2385, 2004) indicates that AP, CO, and Pla are determined by an equilibrium of the pumping ability of the left heart ($S_L$), stressed blood volume (V), and systemic arterial resistance (R). Our system directly controls $S_L$ with dobutamine, V with dextran/furosemide, and R with nitroprusside, thereby controlling the three variables. We evaluated the efficacy of our system in 12 anesthetized dogs with acute decompensated heart failure. Once activated, the system restored $S_L$, V, and R within 30 min, resulting in the restoration of normal AP, CO, and Pla. Steady-state deviations from target values were small for AP [4.4 mmHg (SD 2.6)], CO [5.4 ml·min$^{-1}$·kg$^{-1}$ (SD 2.4)] and Pla [0.8 mmHg (SD 0.6)]. In conclusion, by directly controlling the mechanical determinants of circulation, our system has enabled simultaneous control of AP, CO, and Pla with good accuracy and stability.

computers; negative feedback; circulatory equilibrium

IN THE MANAGEMENT OF PATIENTS with acute decompensated heart failure after myocardial infarction or after cardiac surgical procedures, cardiovascular agents such as inotropes and/or vasodilators are commonly used to control systemic arterial pressure (AP), cardiac output (CO), and left heart filling pressure (2, 13, 20). Because responses to these agents vary between patients and within patient over time, strict monitoring of patient condition and frequent adjustments of drug infusion rates are usually required. This is a difficult and time-consuming process, especially in hemodynamically unstable patients. Several closed-loop systems to automate drug infusion have been developed to facilitate this process (10, 11, 18, 26, 27). Closed-loop control of AP with vasodilators was more precise and stable than manual controls (10, 11). Chitwood et al. (10) demonstrated that, compared with manual control, closed-loop control of postoperative hypertension significantly improves patient outcome by reducing the transfusion requirement and postoperative blood loss. Although closed-loop control of hemodynamics has been suggested to be useful in clinical settings, no closed-loop system so far developed is capable of controlling the overall hemodynamics; i.e., controlling AP, CO, and left heart filling pressure simultaneously (18). This is because all previous systems attempted to directly control the hemodynamic variable by estimating response of the variable to drug infusion (10, 11, 18, 26, 27). Although such an approach worked well in controlling a single variable, it cannot be applied to control of the three variables, because it is difficult to simultaneously estimate their responses to the infusions of multiple drugs.

In this study, we developed a new automated drug delivery system that is capable of controlling AP, CO, and left atrial pressure (Pla). We modeled the entire cardiovascular system by extending Guyton's framework of circulatory equilibrium (16, 17, 24, 25). As shown in Fig. 1, the extended framework consists of an integrated cardiac output curve characterizing the pumping ability of the left and the right heart and a venous return surface characterizing the venous return property of the systemic and pulmonary circulation (24, 25). The intersection point of the integrated CO curve and the venous return surface predicts the equilibrium point of CO, Pla, and right atrial pressure (Pra) (Fig. 1) (24, 25). Once CO, Pla, and Pra are predicted from the intersection point, systemic arterial resistance determines AP. On the basis of this framework, instead of directly controlling AP, CO, and Pla, our system controls the integrated CO curve with dobutamine (Dob), the venous return surface with 10% dextran 40 (Dex) and furosemide (Fur), and systemic arterial resistance with sodium nitroprusside (SNP), thereby controlling the three hemodynamic variables.

Address for reprint requests and other correspondence: K. Uemura, Dept. of Cardiovascular Dynamics, National Cardiovascular Center Research Institute, 5-7-1 Fujishirodai, Suita 565-8565, Japan (e-mail: kuemura@ri.ncvc.go.jp).

The costs of publication of this article were defrayed in part by the payment of page charges. The article must therefore be hereby marked "*advertisement*" in accordance with 18 U.S.C. Section 1734 solely to indicate this fact.

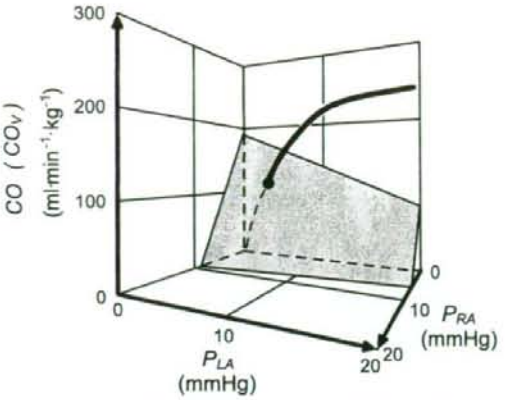


Fig. 1. Diagram of circulatory equilibrium for cardiac output (CO), venous return ($CO_V$), left atrial pressure (Pla), and right atrial pressure (Pra). The equilibrium CO, Pla, and Pra are obtained as the intersection point of the venous return surface and integrated cardiac output curve. [Modified from Uemura et al. (Ref 25).]

The purpose of this study was, therefore, to develop and validate the new automated drug delivery system. We evaluated the efficacy of our system in a canine model of acute ischemic heart failure. Our results indicated that this novel automated drug delivery system was able to control AP, CO, and Pla simultaneously with reasonably good accuracy and stability.

## METHODS

### *Cardiac Output Curve, Venous Return Surface, and Arterial Resistance*

On the basis of previous studies, we parameterized the integrated CO curve by the pumping ability of the left heart ($S_L$), the venous return surface by total stressed blood volume (V), and the systemic arterial resistance by R (see APPENDIX A) (24, 25). Our system aims to control these cardiovascular parameters to achieve target AP (AP*), target CO (CO*), and target Pla (Pla*).

### *Automated Drug Delivery System*

Figure 2*A* illustrates a block diagram of the automated drug delivery system, using a negative feedback mechanism.

Target values of $S_L$ ($S_L$*), V (V*), and R (R*) are determined according to the AP*, CO*, and Pla* (see APPENDIX B). The subject's $S_L$, V, and R are calculated from the measured AP, CO, Pla, and Pra (Fig. 2*A*). $S_L$, V, and R are compared with $S_L$*, V*, and R*, respectively.

To minimize the difference between $S_L$* and $S_L$ ($\Delta S_L = S_L^* - S_L$) and the difference between R* and R ($\Delta R = R^* - R$), proportional-integral (PI) feedback controllers adjusts infusion rates of Dob and SNP, respectively (Fig. 2*A*). In the PI controller (Fig. 2*B*), $\Delta S_L$ (or $\Delta R$) and the difference integrated with an integral gain ($K_i$) are summed and scaled by a proportional gain ($K_p$) to give the infusion rate of Dob (or SNP). We determined values of $K_i$ and $K_p$ on the

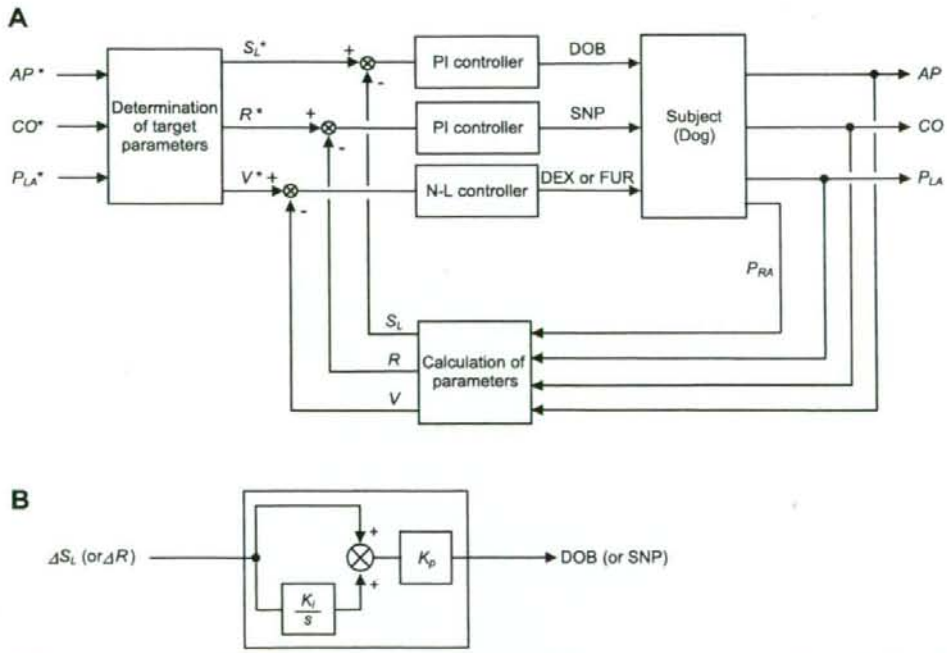


Fig. 2. *A*: block diagram of an automated drug delivery system for simultaneous control of systemic arterial pressure (AP), CO, and Pla. AP*, CO* and Pla* represent target AP, target CO, and target Pla, respectively. From these target variables, target values of pumping ability of the left heart ($S_L$*), stressed blood volume (V*), and systemic arterial resistance (R*) are determined. Subject's $S_L$, V, and R are calculated from measured AP, CO, Pla, and Pra. Proportional-integral (PI) controllers adjust infusion rate of dobutamine (Dob) and sodium nitroprusside (SNP) to minimize the difference between $S_L$ and $S_L$* ($\Delta S_L$), and the difference between R and R* ($\Delta R$), respectively. Nonlinear (N-L) controller adjusts infusion of 10% dextran 40 (Dex) or injection of furosemide (Fur) so that the difference between V and V* is minimized. *B*: block diagram of the PI controller. $K_i$ and $K_p$ represent the integral and proportional gain constants, respectively; $s$ is a Laplace operator.

basis of open-loop response of $S_L$ (or R) to the infusion of Dob (or SNP) (4, 9).

To minimize the difference between V* and V ($\Delta V = V^*-V$), a nonlinear (NL) feedback controller (Fig. 2A) adjusts the infusion of Dex or injection of Fur on the basis of the following "if-then" rules:

Rule 1: If $\Delta V \geq X_1$ ml/kg then infuse Dex ($Y_1$, ml/min)

Rule 2: If $\Delta V \leq X_2$ ml/kg then inject Fur ($Y_2$, mg)

We determined values of $X_1$, $Y_1$, $X_2$, and $Y_2$ on the basis of the open-loop response of V to the infusion of Dex and Fur.

These adjustment processes are repeated in parallel and continued until the differences disappear.

### *Preparation*

We used 35 adult mongrel dogs in this study [both sexes, body weight 25 kg (SD 4)]. Care of the animals was in strict accordance with the guiding principles of the Physiological Society of Japan. All protocols were approved by the Animal Subjects Committee of the National Cardiovascular Center. Anesthesia was induced with pentobarbital sodium (25 mg/kg). Animals were intubated endotracheally. Isoflurane (1.0%) was inhaled continuously to maintain an appropriate level of anesthesia during the experiment. A catheter (8-Fr) was placed in the right femoral artery, which was connected to a pressure transducer (DX-200, Nihon Kohden, Tokyo, Japan) to measure AP. After a median sternotomy, a small pericardial incision was made at the level of the aortic root. Through the incision, an ultrasonic flow meter (20A594, Transonics, Ithaca, NY) was placed around the ascending aorta to measure CO. Fluid-filled catheters were placed in the left and right atria to measure Pla and Pra, respectively. They were connected to pressure transducers (DX-200, Nihon Kohden). The junction between the vena cavae and the right atrium was taken as the reference point for zero pressure. The undamped natural frequency and the damping ratio of the fluid filled catheters for the pressure measurements were 21 Hz and 0.22, respectively. A urinary catheter was inserted to measure urine volume.

A catheter (6-Fr) was placed in the right femoral vein. A roller pump (Minipuls 3, Gilson, Middleton, WI) was attached to the venous line to infuse Dex. A double-lumen catheter was also introduced into the right femoral vein for administration of Dob and SNP. Infusion pumps (CFV-3200, Nihon Kohden) were used for Dob and SNP infusion. The infusion rates of Dex, Dob, and SNP were controlled with a personal computer (MA20V, NEC, Tokyo, Japan) through a 12-bit digital-to-analog converter (DA12-8PCI, Contec, Osaka, Japan). A catheter (6-Fr) was placed in the right external jugular vein, from which Fur was injected after a command signal from the computer.

### *Experimental Protocols*

We induced left ventricular failure (LVF) in all the animals by embolizing the left circumflex coronary artery with glass microspheres (90 μm in diameter) (24, 25). We adjusted the amount of injected microspheres to increase Pla to more than 18 mmHg or decrease CO to less than 70 $ml \cdot min^{-1} \cdot kg^{-1}$. When ventricular tachycardia or frequent premature ventricular contractions were noted, lidocaine (1 mg/min) was infused to suppress the arrhythmia.

*Response of cardiovascular parameters to drug infusion.* Under open-loop conditions, we examined the response of cardiovascular parameters to drug infusions in 21 dogs with LVF. In 10 dogs, we infused Dob in a stepwise manner at 6 $\mu g \cdot kg^{-1} \cdot min^{-1}$ for 10 min to obtain a step response of $S_L$. In six dogs, we infused SNP at 2 $\mu g \cdot kg^{-1} \cdot min^{-1}$ for 10 min to obtain a step response of R. In five dogs, we infused Dex at 0.4 $ml \cdot min^{-1} \cdot kg^{-1}$ for 10 min to observe the response of V. In seven dogs, we injected Fur (20 mg, bolus iv) and observed the response of V and urine volume for 50 min.

*Application of the automated drug delivery system.* We applied the system to the other 14 dogs with LVF. We first defined AP* (90–105 mmHg), CO* (90–100 $ml \cdot min^{-1} \cdot kg^{-1}$), and Pla* (8–12 mmHg), which were fed into the system to determine $S_L$*, V*, and R* (see APPENDIX B). The controllers were then activated by closing the loops. In 12 dogs (*group 1*), we observed the performance of the system over 50–60 min. In two dogs (*group 2*), we observed the performance of the system over 100–150 min to evaluate stability of the closed-loop control over a longer periods of time.

With the use of the computer, analog signals of AP, CO, Pla, and Pra were digitized at 200 Hz with a 12-bit analog-to-digital converter [AD12-16U(PCI)E, Contec, Osaka, Japan] and stored on a hard disk for offline analysis. In the closed-loop control, the digitized signals were smoothed by a low-pass filter (time constant, 10 s) and were used as the system controlled variables. The infusion rates of Dob, SNP, and Dex were also stored. Urine volume after the injection of Fur was recorded.

### *Data Analysis*

*Evaluation of the response of cardiovascular parameters and design of the controller.* We described the step response of $S_L$ and R by a transfer function of a first-order model with a transport delay. In this model, change in $S_L$ from baseline ($\delta S_L$) in response to Dob infusion can be expressed by the following formula:

$$\delta S_L(t) = \begin{cases} G \cdot \left[1 - \exp\left(-\dfrac{t-L}{T}\right)\right] & (t \geq L) \\ 0 & (t < L) \end{cases} \qquad (1)$$

where $G$ is static gain [$ml \cdot min^{-1} \cdot kg^{-1} (\mu g \cdot kg^{-1} \cdot min^{-1})^{-1}$], $L$ is transport delay (s), and $T$ is time constant (s). Change in R from baseline ($\delta R$) in response to the SNP infusion can be expressed similarly and is characterized by $G$ [$mmHg \cdot min \cdot ml^{-1} \cdot kg (\mu g \cdot kg^{-1} \cdot min^{-1})^{-1}$], $L$ (s), and $T$ (s). We estimated the parameters of the transfer function by approximating $\delta S_L$ and $\delta R$ to *Eq. 1* using the least square method. We averaged the parameters of the transfer function of $S_L$ response for 10 animals and those of R response for 6 animals. The averaged parameters were used to determine the PI gain constants, $K_i$ and $K_p$, in accordance with the method of Chien et al. (9). Their method provides PI constants that permit the regulated variable to respond rapidly without overshoot (4, 9).

We evaluated the change in V from baseline ($\delta V$) in response to the infusion of Dex and Fur. On the basis of $\delta V$, we determined the constants ($X_1$, $Y_1$, $X_2$, and $Y_2$) of the if-then rules.

*Efficacy of the automated drug delivery system.* We calculated the following indexes to evaluate the accuracy and stability of the control of AP, CO, and Pla by the new system: the time required for the hemodynamic variables to reach the acceptable ranges of the target values (±10 mmHg for AP, ±10 $ml \cdot min^{-1} \cdot kg^{-1}$ for CO, ±2 mmHg for Pla), and the standard deviations of the steady-state differences between AP and AP*, between CO and CO*, and between Pla and Pla*. Because steady states were reached within 30 min in all the variables in the present study, standard deviations were calculated from 30 min after the loop was closed.

### *Statistics*

Group data are expressed as means (SD) unless otherwise stated. Student's paired $t$-test was used to compare hemodynamic data at baseline and after the coronary embolization. One-way ANOVA with Tukey's post hoc test was used to compare hemodynamic data before, during, and after the closed-loop control of hemodynamics. The level of statistical significance was defined as $P < 0.05$.

## RESULTS

Hemodynamic data at baseline and after left circumflex coronary artery embolization are summarized in Table 1. Coronary embolization more than doubled Pla [from 7.5 (SD 1.9) to 19.4 (SD 6.2) mmHg] and halved CO [from 131.4 (SD

Table 1. *Hemodynamic data at baseline and after left circumflex coronary artery embolization*

| | Baseline | Embolization |
|---|---|---|
| HR, beats/min | 141.3 (19.5) [112.0–188.3] | 146.2 (28.8) [81.4–197.9] |
| AP, mmHg | 109.1 (18.7) [76.4–140.0] | 90.9 (16.5) [66.9–135.6]* |
| CO, ml·min$^{-1}$·kg$^{-1}$ | 131.4 (40.9) [64.5–229.2] | 66.8 (23.3) [30.3–121.7]* |
| *Pla*, mmHg | 7.5 (1.9) [4.7–12.8] | 19.4 (6.2) [7.9–34.5]* |
| *Pra*, mmHg | 4.2 (1.2) [2.1–7.2] | 6.0 (1.8) [3.5–9.9]* |
| $S_L$, ml·min$^{-1}$·kg$^{-1}$ | 54.3 (18.1) [25.2–105.9] | 19.1 (7.6) [8.0–33.7]* |
| R, mmHg·min·ml$^{-1}$·kg | 0.9 (0.4) [0.4–1.8] | 1.4 (0.5) [0.7–2.6]* |
| V, ml/kg | 31.0 (6.6) [21.7–45.2] | 32.3 (4.9) [20.6–43.7] |

Values are means (SD) ($n$ = 35 in each group). Numbers in brackets are the ranges. HR, heart rate. AP, systemic arterial pressure; CO, cardiac output; Pla, left atrial pressure; Pra, right atrial pressure; $S_L$, pumping ability of the left heart; R, systemic arterial resistance; V, stressed blood volume. *$P < 0.01$ vs. baseline.

40.9) to 66.8 (SD 23.3) ml·min$^{-1}$·kg$^{-1}$]. This decreased $S_L$ to about one-third of the baseline value, which indicates substantial downward shift of the left cardiac output curve. These changes are compatible with severe LVF.

*Response of Cardiovascular Parameters to Drug Infusion*

Figure 3 shows the open-loop responses of cardiovascular parameters to drug infusions. Figure 3, *A* and *B*, shows the averaged time course of $\delta S_L$ during Dob infusion ($n$ = 10) and that of $\delta R$ during SNP infusion ($n$ = 6), respectively. Dob infusion increased $\delta S_L$, and SNP infusion decreased $\delta R$ exponentially. The results of the fit of $\delta S_L$ and $\delta R$ to *Eq. 1* are summarized in Table 2. The fact that the correlation coefficients were close to unity, with a small standard error of the estimate relative to the amount of $\delta S_L$ and $\delta R$, suggested that the approximation of $\delta S_L$ and $\delta R$ to *Eq. 1* was reasonably accurate. On the basis of the averaged parameters of the transfer function (Table 2), we determined the PI gain constants for Dob infusion [$K_i$ = 0.01 s$^{-1}$, $K_p$ = 0.06 μg·kg$^{-1}$·min$^{-1}$ (ml·min$^{-1}$·kg$^{-1}$)$^{-1}$] and for SNP infusion [$K_i$ = 0.007 s$^{-1}$, $K_p$ = −1.37 μg·kg$^{-1}$·min$^{-1}$ (mmHg·min·ml$^{-1}$·kg)$^{-1}$].

Figure 3*C* shows the averaged time course of δV in response to Dex infusion ($n$ = 5). δV increased and plateaued [7.2 ml/kg (SD 2.2)] after the cessation of Dex infusion. δV at the plateau was greater than the total volume of Dex infused (4 ml/kg), suggesting transvascular fluid absorption by colloid osmotic pressure (3). Figure 3*D* shows the averaged time course of δV after a single intravenous injection of Fur (20 mg, $n$ = 7). δV gradually decreased and reached a trough [−4.3 ml/kg (SD 3.5)] around 30 min after the Fur injection. Average urine volume was 180 ml (SD 94). On the basis of these responses, we determined the constants of the if-then rules as $X_1$ = 1 ml/kg, $Y_1$ = 10 ml/min, $X_2$ = −2 ml/kg, and $Y_2$ = 10 mg. To avoid oscillation between hypovole-

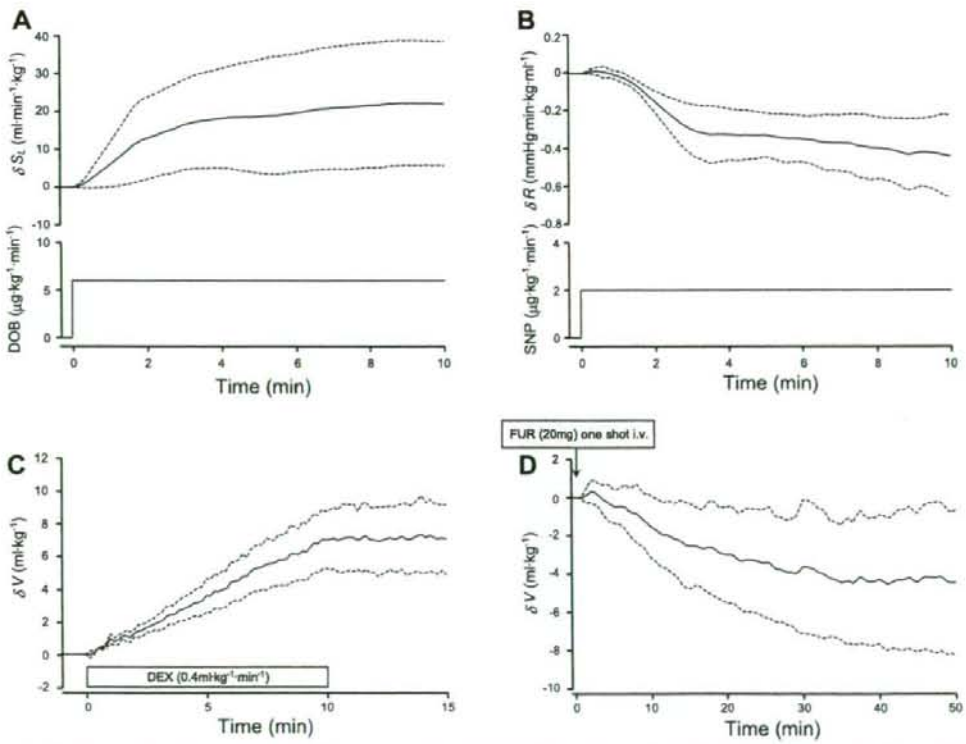


Fig. 3. Response of cardiovascular parameter to drug infusion. *A*: averaged response of $S_L$ to stepwise Dob infusion (6 μg·kg$^{-1}$·min$^{-1}$) ($n$ = 10). The ordinate indicates change in $S_L$ from baseline ($\delta S_L$). *B*: averaged response of R to stepwise SNP infusion (2 μg·kg$^{-1}$·min$^{-1}$) ($n$ = 6). The ordinate indicates change in R from baseline (δR). *C* and *D*: averaged response of V to Dex infusion (0.4 ml·min$^{-1}$·kg$^{-1}$) (*C*, $n$ = 5) and to Fur (20 mg) injection (*D*, $n$ = 7). The ordinates indicate change in V from baseline (δV). Data are expressed by mean (solid line) ± SD (broken line).

Table 2. *Parameters of step response of $S_L$ and R*

| | *G* | *L* | *T* | *r* | SEE |
|---|---|---|---|---|---|
| $\delta S_L$ | 3.6 (2.7) | 63.5 (46.9) | 79.0 (78.0) | 0.91 (0.09) | 2.0 (0.7) |
| $\delta R$ | −0.21 (0.08) | 69.8 (26.1) | 117.1 (80.2) | 0.93 (0.02) | 0.06 (0.02) |

Values are means (SD). $\delta S_L$, change in $S_L$ from baseline; $\delta R$, change in R from baseline; *G*, static gain of $\delta S_L$ [ml·min$^{-1}$·kg$^{-1}$ (μg·kg$^{-1}$·min$^{-1}$)$^{-1}$] and of $\delta R$ [mmHg·min·ml$^{-1}$·kg (μg· kg$^{-1}$·min$^{-1}$)$^{-1}$]; *L*, transport delay (s); *T*, time constant (s); *r*, correlation coefficient; SEE, standard error of the estimate of $\delta S_L$ (ml·min$^{-1}$·kg$^{-1}$) and of $\delta R$ (mmHg·min·ml$^{-1}$·kg).

mia and hypervolemia (hence infusion of Dex and injection of Fur), we introduced a dead zone ($-2$ ml/kg $< \Delta V <$ 1 ml/kg) into the rules (4). We set continuous checking for *rule 1* and checking at 20-min intervals for *rule 2*.

With the controllers thus designed, we evaluated the performance of the automated system in the next protocol.

*Performance of the Automated Drug Delivery System*

Figure 4 shows the experimental trial in a representative case. The automated system was activated at 0 min. Figure 4*A* shows the time courses of the infusion rates of Dob and SNP and the accumulated volume of infused Dex. In this case, Fur was not injected. Figure 4*B* shows the time courses of $S_L$, R, and V. Infusion rates of Dob, SNP, and Dex were adjusted so that $S_L$, R, and V reached their respective target values. By controlling the cardiovascular parameters, the automated system controlled AP, CO, and Pla accurately and stably as demonstrated in Fig. 4*C*. AP, CO, and Pla reached their respective target levels within 30 min and remained at these levels.

Figure 5 summarizes the results obtained for 12 dogs (*group 1*), demonstrating the effectiveness of the performance of the automated system. Figure 5*A* shows averaged time courses of the infusion rates of Dob and SNP, and the accumulated volume of infused Dex. The average infusion rates of Dob and SNP were 4.7 μg·kg$^{-1}$·min$^{-1}$ (SD 2.6) and 4.2 μg·kg$^{-1}$·min$^{-1}$ (SD 1.8), respectively. The average volume of infused Dex was 2.4 ml/kg (SD 1.9). Fur was injected once in one animal and twice in another animal. In these two animals, V decreased by 3.8–10.2 ml/kg in response to the injection of Fur with a total urine volume of 250–300 ml. Figure 5*B* shows averaged time courses of difference between $S_L$ and $S_L$* ($S_L - S_L$*), difference between R and R* (R − R*), and difference between V and V* (V − V*). Once the system was activated, these differences rapidly converged to the zero lines in all the animals. $S_L$ was restored to subnormal conditions [33.0 ml·min$^{-1}$·kg$^{-1}$ (SD 2.6)] irrespective of the magnitude of depression before the control [13.8 ml·min$^{-1}$·kg$^{-1}$ (SD 3.5), from 9.4 to 20.5 ml·min$^{-1}$·kg$^{-1}$]. These resulted in accurate and stable control of AP, CO, and Pla (Fig. 5*C*). The ordinates of Fig. 5*C* indicate the difference between AP and AP* (AP − AP*), difference between CO and CO* (CO − CO*), and difference between Pla and Pla* (Pla − Pla*). These differences also converged to the zero lines rapidly. The average times for AP, CO, and Pla to reach the acceptable ranges were 5.2 min (SD 6.6), 6.8 min (SD 4.6), and 11.7 min (SD 9.8),

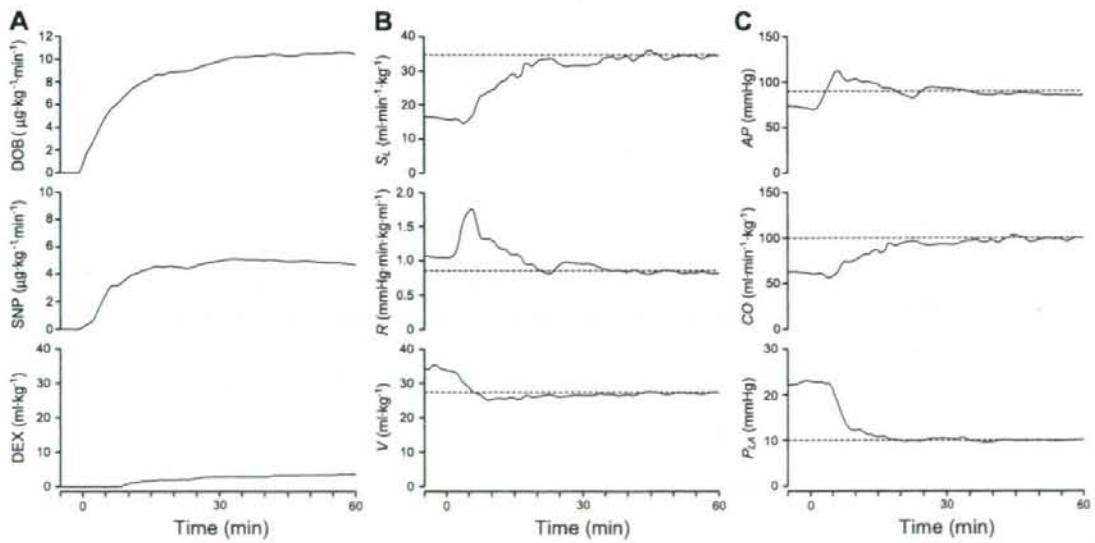


Fig. 4. Time courses of infusion rates of Dob and SNP, and cumulated volume of infused Dex (*A*), cardiovascular parameters (*B*), and hemodynamic variables (*C*) in 1 representative animal during closed-loop control of hemodynamics. Broken horizontal lines in *B* indicate target parameters (*top*, $S_L$*; *middle*, R*; *bottom*, V*). Broken horizontal lines in *C* indicate target hemodynamic variables (*top*, AP*; *middle*, CO*; *bottom*, Pla*). Drug infusion rates were adjusted so that the cardiovascular parameters reached the respective target values. As the parameters got closer to their targets, all 3 hemodynamic variables approached their respective target values.

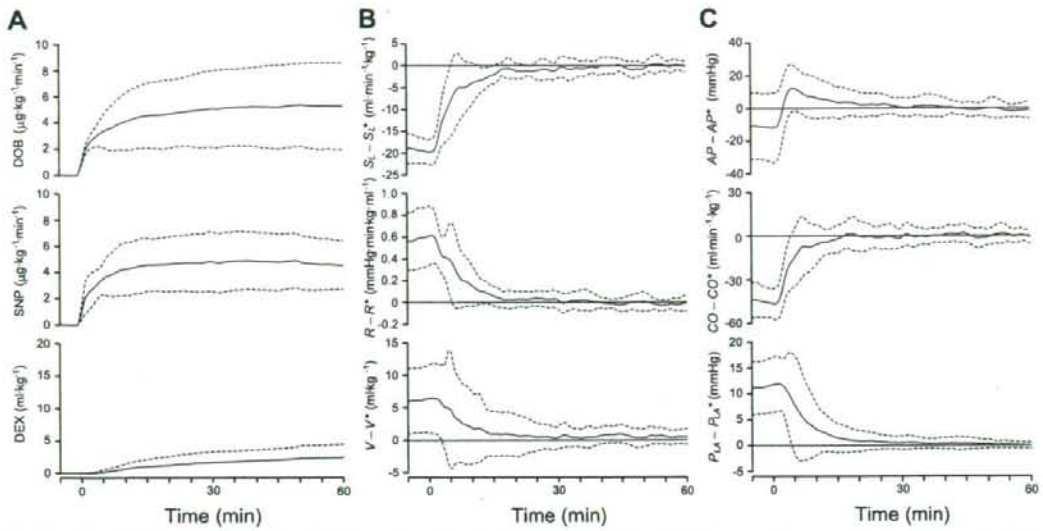


Fig. 5. Time courses of infusion rates of Dob and SNP, and cumulated volume of infused Dex (*A*), differences between measured and target cardiovascular parameters (*B*), and differences between measured and target hemodynamic variables (*C*) averaged for 12 dogs during closed-loop control of hemodynamics. Data are expressed as mean (solid line) ± SD (broken line). As the differences between measured and target parameters converged to the zero lines, the differences between measured and target hemodynamic variables also converged to the zero lines and remained at those levels.

respectively. The average standard deviations from the target values were small for AP [4.4 mmHg (SD 2.6)], CO [5.4 $ml \cdot min^{-1} \cdot kg^{-1}$ (SD 2.4)] and Pla [0.8 mmHg (SD 0.6)]. In case of severe hypotension, restoring normal AP should be done within a few minutes to prevent cerebral ischemia. Four of 12 dogs exhibited severe hypotension [AP, 67 mmHg (SD 6)]. In these animals, AP* [95 mmHg (SD 4)] was attained within 4 min [mean 2.8 min (SD 0.7)]. Hemodynamic data before, during, and after the closed-loop control of hemodynamics are summarized in Table 3. After the system was turned off, AP, CO, and Pla gradually returned to their precontrol levels in 11 animals. In one animal, however, progressive hypotension followed by intractable ventricular fibrillation occurred ~3 min after the system was turned off.

In two dogs (*group 2*), AP, CO, and Pla were controlled with reasonable stability over a longer periods of time (100–150 min). Standard deviations from target values were small for AP (3.9–7.8 mmHg), CO (2.7–6.6 $ml \cdot min^{-1} \cdot kg^{-1}$), and Pla (0.7–2.5 mmHg).

Table 3. *Hemodynamic data before, during, and after the closed-loop control of hemodynamics*

| | Before ($n$ = 12) | During ($n$ = 12) | After ($n$ = 11) |
|---|---|---|---|
| HR, beats/mm | 147.4 (26.8) | 149.4 (25.0) | 135.7 (25.2)†‡ |
| AP, mmHg | 86.7 (22.4) | 97.0 (7.4) | 75.2 (21.1)‡ |
| CO, $ml \cdot min^{-1} \cdot kg^{-1}$ | 53.7 (14.6) | 96.7 (5.3)† | 53.5 (8.6)‡ |
| *Pla*, mmHg | 21.8 (5.5) | 10.8 (1.2)† | 18.5 (3.4)‡ |
| *Pra*, mmHg | 6.9 (1.8) | 4.4 (0.9)† | 7.4 (2.2)‡ |
| $S_L$, $ml \cdot min^{-1} \cdot kg^{-1}$ | 14.3 (4.0) | 32.7 (2.6)† | 15.1 (2.9)‡ |
| R, $mmHg \cdot min \cdot ml^{-1} \cdot kg$ | 1.5 (0.3) | 1.0 (0.1)† | 1.3 (0.4)*‡ |
| V, ml/kg | 34.2 (4.9) | 28.5 (2.3)† | 34.0 (5.4)‡ |

Values are means (SD). *$P < 0.05$, †$P < 0.01$ vs. Before; ‡$P < 0.01$ vs. During.

## DISCUSSION

To the best of our knowledge, the automated drug delivery system we have developed is the first to successfully control AP, CO, and Pla simultaneously with reasonably good accuracy and stability. In a canine model of acute heart failure, our system automatically normalizes AP, CO, and Pla and maintains the levels stably within the desired ranges. Therefore, our system is potentially useful in the management of patients with acute decompensated heart failure.

### *Previous Closed-Loop Systems Controlling Hemodynamic Variables*

Several previous systems have attempted to control two hemodynamic variables simultaneously (18, 26, 27). However, it is difficult to expand them to closed-loop control of the overall hemodynamics.

Voss et al. (26) and Yu et al. (27) reported closed-loop systems to control AP and CO using inotropes and vasodilators in dogs. In these systems, all possible input-output relations between drug infusion and the response of the controlled variable have to be estimated; namely, inotrope-AP, inotrope-CO, vasodilator-AP, and vasodilator-CO relations. The reason for this is that these drugs affect AP and CO simultaneously to almost the same degree. If this approach is applied to simultaneous control of AP, CO, and Pla, at least nine input-output relations have to be estimated, because at least three drugs are required to independently control the three variables. This would make the system extremely complicated and therefore be practically unfeasible.

In addition, the input-output relations must be estimated online in individual animals to tune the drug controllers. The reason for this is that the relations differ widely between animals and within animal over time. Even the direction of the

output response can change. For example, CO usually increases in response to SNP infusion in subjects with failing hearts but may also decrease in subjects with preserved cardiac function (23, 26). In the closed-loop system of Voss et al., such estimation induced unacceptably large fluctuations in AP (26). The feasibility of such online estimation is questionable when drug infusion rates are allowed to vary simultaneously because of the difficulty to differentiate between drug effects. To avoid this problem, Hoeksel et al. (18) allowed only one drug to be varied at a time, whereas other drugs were kept constant in closed-loop control of AP and pulmonary arterial pressure during cardiac surgery. However, their adjustments of volume supplementation or dobutamine infusion were manual. Their system did not completely automate the control of hemodynamics.

*Characteristics of Our System*

Our system controls the cardiovascular parameters characterizing the integrated CO curve, venous return surface, and arterial resistance and as a result achieves target values for hemodynamic variables. Compared with previous systems, our system may appear to adopt a rather roundabout approach. Our concept is that controlling the cardiovascular parameters is physiologically more rational, because it is equivalent to directly controlling the mechanical determinants of circulation. As indicated by Guyton et al. (16, 17), when the mechanics of the circulation are considered, the hemodynamic variables such as AP, CO, and atrial pressures are the effects, or dependent variables. Blood volume and the mechanical properties of the heart and vasculature, such as heart rate, ventricular contractility, and vascular resistance, are the causes, or independent variables. The integrated CO curve and venous return surface display these properties through the relationship between the flow and atrial pressures (24, 25). The total artificial heart control system developed by Abe et al. (1) adjusted its output in accordance with the vascular conductance (1/resistance) and AP, thereby achieving appropriate response to peripheral metabolic demands and avoiding hemodynamic abnormalities exhibited by other total artificial heart control systems. Their results also suggest that it is essential to consider the mechanical determinant of circulation for the control of the hemodynamic variables.

Our approach is advantageous from the perspective of control engineering. The three drug controllers (Fig. 2*A*) are designed on the basis of only four input-output relations between the drug infusion and the response of the controlled parameter; namely, Dob-$S_L$, SNP-R, Dex-V, and Fur-V (Fig. 3). We also found that Dob decreases R and increases V, and SNP increases $S_L$ and decreases V (data not shown), which are compatible with previous studies (7, 22, 23). If these secondary effects induce significant interactions among the three closed loops, additional controllers would be needed to compensate for the interactions (4). However, our results indicate that these secondary effects are small enough to be compensated by the three drug controllers, and additional controllers are not necessary. The fact that the three closed loops are effectively decoupled drastically simplifies the entire system. This also permits system operators to understand its behavior easily (4).

Although we fix the PI gain constants and the constants of if-then rules, controls of cardiovascular parameters are accurate and stable (Fig. 4*B*). There are interindividual differences in the response of the parameters to drug infusion (Fig. 3). There should also be intraindividual differences in the response over time. However, our results indicate that the three drug controllers effectively compensate for all of these differences and do not require adaptive tuning in individual animals as in the previous system. As long as each cardiovascular parameter responds sensitively to the corresponding agent, our system is able to achieve target values for all the parameters, thereby achieving target hemodynamic variables.

Our system explicitly quantifies cardiac pump function, preload, and afterload, thereby controlling the overall hemodynamics. We believe that this unique feature of our system is intuitively appealing and is acceptable to clinicians.

*Clinical Application of Our System*

Our system will reduce the stress and work imposed on physicians and nurses who are managing patients with unstable hemodynamic conditions. These personnel will be able to spend more time on other patient-related activities, thereby improving the quality of patient care (10, 11). We believe that the closed-loop control of overall hemodynamics can extend the improvement in postoperative outcome demonstrated by Chitwood et al. (10) to various aspects of clinical cardiology or cardiac surgery.

In clinical settings, multisystem disorders such as renal disease, anemia, and diabetes may affect the performance of our system. Renal disease can weaken the response of V to the infusion of Fur. The hemodynamic changes in anemia include increased preload and reduced arterial resistance as compensatory mechanisms for the reduced oxygen-carrying capacity of the blood (8). These changes may affect the control of V and R by our system. In patients with diabetic cardiomyopathy, the sensitivity of $S_L$ to Dob infusion may be reduced (5). Drugs prescribed before hospitalization such as β-blockers, or used during hospitalization such as morphine may also affect the performance of our system. Chronic β-adrenergic blockade can weaken the sensitivity of $S_L$ to Dob infusion (2). Administration of morphine may change the response of V and R to the drugs infused (15). We must clarify these effects on the performance of our system as thoroughly as possible before our system can be considered for clinical application.

In the routine clinical environment, CO, and pulmonary artery occlusion pressure, a substitute for Pla, are measured intermittently with a Swan-Ganz catheter. For clinical application of our system, it is a prerequisite to monitor these variables continuously. Several methods have been developed to continuously monitor CO or the pulmonary artery occlusion pressure (6, 12). Integrating these methods into our system would bring the clinical application of our system closer to reality.

*Limitations*

All the experiments of this study were conducted in anesthetized, open-chest dogs. Anesthesia and surgical trauma affect the cardiovascular system significantly. Whether the present system is efficacious in conscious, closed-chest animals (including humans) remains to be seen.

We parameterized the integrated cardiac output curve and the venous return surface using *Eqs. A1*, *A2*, and *A4* (24, 25). Even if the actual curve or surface deviate slightly from those

estimated by these equations, our system compensates such deviations by the negative feedback mechanism. However, we did not confirm whether the estimation works well outside the physiological ranges of Pla and Pra, particularly under low atrial pressures (24, 25). The efficacy of our system in such conditions remains to be evaluated.

Our system controls R with vasodilators only and lacks a controller to increase R with vasoconstrictors. This will not be a major problem because the pathophysiology of acute heart failure is characterized by excessive vasoconstriction due to enhanced activity of sympathetic and renin-angiotensin systems (19). Vasoconstrictor control is necessary, however, for the management of patients with excessive vasodilatation, such as those in septic shock (21).

In this study, control of $S_L$ was accurate and stable. However, it would be impossible to restore $S_L$ pharmacologically if $S_L$ is more severely depressed than those seen in this study as in the case of more diffuse myocardial disease or superimposed coronary artery disease. We must clarify in future studies to what magnitude of $S_L$ depression can our system restore it reliably. In addition, how to use our system with mechanical circulatory support such as the intra-aortic balloon pump in case of the severe $S_L$ depression remains to be established.

In the present design, if $S_L$ is unable to respond to the infusion of Dob, the system will automatically increase the infusion rate of Dob owing to its negative feedback mechanism. This would be problematic especially in case of arrhythmia, which is a serious noise in the closed-loop control of $S_L$. If not appropriately suppressed, frequent premature ventricular contractions or ventricular tachycardia will depress $S_L$ owing to disorganized ventricular contraction. In response to the depressed $S_L$, the system automatically increases the infusion rate of dobutamine. This could further exacerbate the arrhythmia, thus leading to a vicious cycle and collapse of the hemodynamics. To prevent such malfunction, a smart "sensor" that will filter these unwanted artifacts should be included in our system.

In the present study, we recorded only the urine volume. Measurement of urine flow and sodium excretion is essential to evaluate renal function, which is a very important prognostic indicator in patients with acute decompensated heart failure (14). It would be desirable to add the monitoring of these parameters to our system to improve the quality of patient care.

In conclusion, by directly controlling the mechanical determinants of circulation, our automated drug delivery system allows simultaneous control of AP, CO, and Pla with reasonable accuracy and stability and is potentially a powerful clinical tool for the management of patients with acute decompensated heart failure.

## APPENDIX A

### *Parameters of Integrated Cardiac Output Curve, Venous Return Surface, and Arterial Resistance*

We parameterized the integrated CO curve, the venous return surface and the systemic arterial resistance on the basis of previous studies (24, 25). In the integrated CO curve, CO ($ml \cdot min^{-1} \cdot kg^{-1}$) is closely related to Pla (mmHg) by the following formula (24):

$$CO = S_L \times [\ln(Pla - 2.03) + 0.80] \quad (A1)$$

and CO to Pra (mmHg) as follows:

$$CO = S_R \times [\ln(Pra - 1.0) + 0.88] \quad (A2)$$

$S_L$ and $S_R$ ($ml \cdot min^{-1} \cdot kg^{-1}$) are parameters representing the preload sensitivity of CO, i.e., the pumping ability of the left and right heart, respectively. These relations are consistent among different animals (24). In a preliminary study, we found that the ratio of $S_R$ to $S_L$ ($\alpha$) remains fairly constant during infusion of dobutamine (data not shown). This suggests that once we know $\alpha$, we can predict $S_R$ in relation to a known change in $S_L$. Therefore we used $S_L$ to parameterize the integrated CO curve. $S_L$ can be calculated from CO and Pla by rewriting *Eq. A1* as follows:

$$S_L = CO/[\ln(Pla - 2.03) + 0.80] \quad (A3)$$

The venous return surface can be mathematically expressed by the following formula (25):

$$CO_V = V/0.129 - 19.61Pra - 3.49Pla \quad (A4)$$

V (ml/kg) is total stressed blood volume, and $CO_V$ ($ml \cdot min^{-1} \cdot kg^{-1}$) is integrated venous return from systemic and pulmonary circulations. This relationship is also consistent among different animals (25). We used V to parameterize the venous return surface. V can be calculated from CO (= $CO_V$), Pla, and Pra by rewriting *Eq. A4* as follows:

$$V = (CO + 19.61Pra + 3.49Pla) \times 0.129 \quad (A5)$$

We parameterized the systemic arterial resistance (R) ($mmHg \cdot ml^{-1} \cdot min \cdot kg$) by the following formula:

$$R = (AP - Pra)/CO \quad (A6)$$

## APPENDIX B

### *Determination of Target Parameters*

On the basis of AP*, CO*, and Pla*, our system determines $S_L$*, V*, and R* as follows: $S_L$* is calculated by substituting CO* and Pla* into *Eq. A3*. By substituting baseline CO, Pla, and Pra into *Eqs. A1* and *A2*, baseline $S_L$ and $S_R$ are calculated to determine $\alpha$. $S_R$ ($S_R$*) corresponding to $S_L$* is predicted as:

$$S_R^* = \alpha \cdot S_L^* \quad (B1)$$

From *Eq. A2* and *B1*, target Pra (Pra*) is predicted as:

$$Pra^* = \exp[(CO^*)/(S_R^*) - 0.88] + 1.0 \quad (B2)$$

By substituting CO*, Pla*, and Pra* into *Eq. A5*, V* can be determined. By substituting AP*, CO*, and Pra* into *Eq. A6*, R* can be calculated.

## GRANTS

This study was supported by Grant-in-Aid for Young Scientists (B) (16700379) from the Ministry of Education, Culture, Sports, Science and Technology, by Health and Labour Sciences Research Grants for Research on Medical Devices for Analyzing, Supporting and Substituting the Function of Human Body (H15-physi-001) from the Ministry of Health Labour and Welfare of Japan, and by the Program for Promotion of Fundamental Studies in Health Science of the National Institute of Biomedical Innovation. This study was also conducted as a part of "Ground-based Research Announcement for Space Utilization" promoted by Japan Space Forum.

## REFERENCES

1. **Abe Y, Chinzei T, Mabuchi K, Snyder AJ, Isoyama T, Imanishi K, Yonezawa T, Matsuura H, Kouno A, Ono T, Atsumi K, Fujimasa I, and Imachi K.** Physiological control of a total artificial heart: conductance- and arterial pressure-based control. *J Appl Physiol* 84: 868–876, 1998.
2. **Antman EM, Anbe DT, Armstrong PW, Bates ER, Green LA, Hand M, Hochman JS, Krumholz HM, Kushner FG, Lamas GA, Mullany CJ, Ornato JP, Pearle DL, Sloan MA, and Smith SC Jr; American College of Cardiology; American Heart Association; Canadian Car-**

**diovascular Society.** ACC/AHA guidelines for the management of patients with ST-elevation myocardial infarction—executive summary. A report of the American College of Cardiology/American Heart Association Task Force on Practice Guidelines (Writing Committee to revise the 1999 guidelines for the management of patients with acute myocardial infarction). *J Am Coll Cardiol* 44: 671–719, 2004.

3. **Arakawa M, Jerome EH, Enzan K, Grady M, and Staub NC.** Effects of dextran 70 on hemodynamics and lung liquid and protein exchange in awake sheep. *Circ Res* 67: 852–861, 1990.
4. **Astrom KJ and Hagglund T.** *PID Controller: Theory, Design, and Tuning* (2nd ed.). Research Triangle Park, NC: Instrument Society of America, 1995, p. 59–199.
5. **Atkins FL, Dowell RT, and Love S.** β-Adrenergic receptors, adenylate cyclase activity, and cardiac dysfunction in the diabetic rat. *J Cardiovasc Pharmacol* 7: 66–70, 1985.
6. **Bein B, Worthmann F, Tonner PH, Paris A, Steinfath M, Hedderich J, and Scholz J.** Comparison of esophageal Doppler, pulse contour analysis, and real-time pulmonary artery thermodilution for the continuous measurement of cardiac output. *J Cardiothorac Vasc Anesth* 18: 185–189, 2004.
7. **Binkley PF, Murray KD, Watson KM, Myerowitz PD, and Leier CV.** Dobutamine increases cardiac output of the total artificial heart. Implications for vascular contribution of inotropic agents to augmented ventricular function. *Circulation* 84: 1210–1215, 1991.
8. **Chapler CK and Cain SM.** The physiologic reserve in oxygen carrying capacity: studies in experimental hemodilution. *Can J Physiol Pharmacol* 64: 7–12, 1986.
9. **Chien KL, Hrones JA, and Reswick JB.** On the automatic control of generalized passive systems. *Trans ASME* 74: 175–185, 1952.
10. **Chitwood WR Jr, Cosgrove DM III, and Lust RM.** Multicenter trial of automated nitroprusside infusion for postoperative hypertension. Titrator Multicenter Study Group. *Ann Thorac Surg* 54: 517–522, 1992.
11. **Cosgrove DM III, Petre JH, Waller JL, Roth JV, Shepherd C, and Cohn LH.** Automated control of postoperative hypertension: a prospective, randomized multicenter study. *Ann Thorac Surg* 47: 678–682, 1989.
12. **DeBoisblanc BP, Pellett A, Johnson R, Champagne M, McClarty E, Dhillon G, and Levitzky M.** Estimation of pulmonary artery occlusion pressure by an artificial neural network. *Crit Care Med* 31: 261–266, 2003.
13. **Forrester JS, Diamond G, Chatterjee K, and Swan HJ.** Medical therapy of acute myocardial infarction by application of hemodynamic subsets (first of two parts). *N Engl J Med* 295: 1356–1362, 1976.
14. **Gottlieb SS, Abraham W, Butler J, Forman DE, Loh E, Massie BM, O'Connor CM, Rich MW, Stevenson LW, Young J, and Krumholz HM.** The prognostic importance of different definitions of worsening renal function in congestive heart failure. *J Card Fail* 8: 136–141, 2002.
15. **Greenberg S, McGowan C, Xie J, and Summer WR.** Selective pulmonary and venous smooth muscle relaxation by furosemide: a comparison with morphine. *J Pharmacol Exp Ther* 270: 1077–1085, 1994.
16. **Guyton AC.** Determination of cardiac output by equating venous return curves with cardiac response curves. *Physiol Rev* 35: 123–129, 1955.
17. **Guyton AC, Coleman TG, and Granger HJ.** Circulation: overall regulation. *Annu Rev Physiol* 34: 13–46, 1972.
18. **Hoeksel SA, Blom JA, Jansen JR, Maessen JG, and Schreuder JJ.** Automated infusion of vasoactive and inotropic drugs to control arterial and pulmonary pressures during cardiac surgery. *Crit Care Med* 27: 2792–2798, 1999.
19. **Johnson W, Omland T, Hall C, Lucas C, Myking OL, Collins C, Pfeffer M, Rouleau JL, and Stevenson LW.** Neurohormonal activation rapidly decreases after intravenous therapy with diuretics and vasodilators for class IV heart failure. *J Am Coll Cardiol* 39: 1623–1629, 2002.
20. **Kaplan JA and Guffin AV.** Treatment of perioperative left ventricular failure. In: *Cardiac Anesthesia* (3rd ed.), edited by Kaplan JA. Philadelphia, PA: Saunders, 1993, p. 1058–1094.
21. **Martin C, Viviand X, Arnaud S, Vialet R, and Rougnon T.** Effects of norepinephrine plus dobutamine or norepinephrine alone on left ventricular performance of septic shock patients. *Crit Care Med* 27: 1708–1713, 1999.
22. **Ogilvie RI and Zborowska-Sluis D.** Effects of nitroglycerin and nitroprusside on vascular capacitance of anesthetized ganglion-blocked dogs. *J Cardiovasc Pharmacol* 18: 574–580, 1991.
23. **Pouleur H, Covell JW, and Ross J Jr.** Effects of nitroprusside on venous return and central blood volume in the absence and presence of acute heart failure. *Circulation* 61: 328–337, 1980.
24. **Uemura K, Kawada T, Kamiya A, Aiba T, Hidaka I, Sunagawa K, and Sugimachi M.** Prediction of circulatory equilibrium in response to changes in stressed blood volume. *Am J Physiol Heart Circ Physiol* 289: H301–H307, 2005.
25. **Uemura K, Sugimachi M, Kawada T, Kamiya A, Jin Y, Kashihara K, and Sunagawa K.** A novel framework of circulatory equilibrium. *Am J Physiol Heart Circ Physiol* 286: H2376–H2385, 2004.
26. **Voss GI, Katona PG, and Chizeck HJ.** Adaptive multivariable drug delivery: control of arterial pressure and cardiac output in anesthetized dogs. *IEEE Trans Biomed Eng* 34: 617–623, 1987.
27. **Yu C, Roy RJ, Kaufman H, and Bequette BW.** Multiple-model adaptive predictive control of mean arterial pressure and cardiac output. *IEEE Trans Biomed Eng* 39: 765–778, 1992.

*J Appl Physiol* 102: 622–627, 2007.
First published November 2, 2006; doi:10.1152/japplphysiol.00622.2006.

# Hypothermia reduces ischemia- and stimulation-induced myocardial interstitial norepinephrine and acetylcholine releases

**Toru Kawada,[1] Hirotoshi Kitagawa,[2] Toji Yamazaki,[2] Tsuyoshi Akiyama,[2] Atsunori Kamiya,[1] Kazunori Uemura,[1] Hidezo Mori,[2] and Masaru Sugimachi[1]**

[1]*Department of Cardiovascular Dynamics, Advanced Medical Engineering Center, and*
[2]*Department of Cardiac Physiology, National Cardiovascular Center Research Institute, Osaka, Japan*

Submitted 4 June 2006; accepted in final form 1 November 2006

**Kawada T, Kitagawa H, Yamazaki T, Akiyama T, Kamiya A, Uemura K, Mori H, Sugimachi M.** Hypothermia reduces ischemia- and stimulation-induced myocardial interstitial norepinephrine and acetylcholine releases. *J Appl Physiol* 102: 622–627, 2007. First published November 2, 2006; doi:10.1152/japplphysiol.00622.2006.—Although hypothermia is one of the most powerful modulators that can reduce ischemic injury, the effects of hypothermia on the function of the cardiac autonomic nerves in vivo are not well understood. We examined the effects of hypothermia on the myocardial interstitial norepinephrine (NE) and ACh releases in response to acute myocardial ischemia and to efferent sympathetic or vagal nerve stimulation in anesthetized cats. We induced acute myocardial ischemia by coronary artery occlusion. Compared with normothermia ($n = 8$), hypothermia at 33°C ($n = 6$) suppressed the ischemia-induced NE release [63 nM (SD 39) vs. 18 nM (SD 25), $P < 0.01$] and ACh release [11.6 nM (SD 7.6) vs. 2.4 nM (SD 1.3), $P < 0.01$] in the ischemic region. Under hypothermia, the coronary occlusion increased the ACh level from 0.67 nM (SD 0.44) to 6.0 nM (SD 6.0) ($P < 0.05$) and decreased the NE level from 0.63 nM (SD 0.19) to 0.40 nM (SD 0.25) ($P < 0.05$) in the nonischemic region. Hypothermia attenuated the nerve stimulation-induced NE release from 1.05 nM (SD 0.85) to 0.73 nM (SD 0.73) ($P < 0.05$, $n = 6$) and ACh release from 10.2 nM (SD 5.1) to 7.1 nM (SD 3.4) ($P < 0.05$, $n = 5$). In conclusion, hypothermia attenuated the ischemia-induced NE and ACh releases in the ischemic region. Moreover, hypothermia also attenuated the nerve stimulation-induced NE and ACh releases. The Bezold-Jarisch reflex evoked by the left anterior descending coronary artery occlusion, however, did not appear to be affected under hypothermia.

vagal nerve; sympathetic nerve; cardiac microdialysis; cats

HYPOTHERMIA IS ONE OF THE most powerful modulators that can reduce ischemic injury in the central nervous system, heart, and other organs. The general consensus is that hypothermia induces a hypometabolic state in tissues and balances energy supply and demand (25). With respect to the myocardial ischemia, the size of a myocardial infarction correlates with temperature (6), and mild hypothermia can protect the myocardium against acute ischemic injury (9). The effects of hypothermia on the function of the cardiac autonomic nerves in terms of neurotransmitter releases, however, are not fully understood. Because autonomic neurotransmitters such as norepinephrine (NE) and ACh directly impinge on the myocardium, they would be implicated in the cardioprotection by hypothermia.

In previous studies from our laboratory, Kitagawa et al. (16) demonstrated that hypothermia attenuated the nonexocytotic NE release induced pharmacologically by ouabain, tyramine, or cyanide. Kitagawa et al. (15) also demonstrated that hypothermia attenuated the exocytotic NE release in response to vena cava occlusion or to local administration of high $K^+$. The effects of hypothermia on the ischemia-induced myocardial interstitial NE release, however, were not examined in those studies. In addition, the effects of hypothermia on the ischemia-induced myocardial interstitial ACh release have never been examined. Because both sympathetic and parasympathetic nerves control the heart, simultaneous monitoring of the myocardial interstitial releases of NE and ACh (14, 31) would help integrative understanding of the autonomic nerve terminal function under hypothermia in conjunction with acute myocardial ischemia.

In the present study, the effects of hypothermia on the ischemia-induced and nerve stimulation-induced myocardial interstitial neurotransmitter releases were examined. We implanted a dialysis probe into the left ventricular free wall of anesthetized cats and measured dialysate NE and ACh levels as indexes of neurotransmitter outputs from the cardiac sympathetic and vagal nerve terminals, respectively. Based on our laboratory's previous results (15, 16), we hypothesized that hypothermia would attenuate the neurotransmitter releases in response to acute myocardial ischemia and to electrical nerve stimulation.

## MATERIALS AND METHODS

### *Surgical Preparation and Protocols*

Animals were cared for in accordance with the *Guiding Principles for the Care and Use of Animals in the Field of Physiological Sciences*, approved by the Physiological Society of Japan. All protocols were reviewed and approved by the Animal Subjects Committee of National Cardiovascular Center. Adult cats were anesthetized via an intraperitoneal injection of pentobarbital sodium (30–35 mg/kg) and ventilated mechanically through an endotracheal tube with oxygen-enriched room air. The level of anesthesia was maintained with a continuous intravenous infusion of pentobarbital sodium (1–2 $mg \cdot kg^{-1} \cdot h^{-1}$) through a catheter inserted from the right femoral vein. Mean arterial pressure (MAP) was measured using a pressure transducer connected to a catheter inserted from the right femoral artery. Heart rate (HR) was determined from an electrocardiogram.

*Protocol 1: acute myocardial ischemia.* We examined the effects of hypothermia on the ischemia-induced myocardial interstitial releases of NE and ACh. The heart was exposed by partially removing the left fifth and/or sixth rib. A dialysis probe was implanted transversely into

Address for reprint requests and other correspondence: T. Kawada, Dept. of Cardiovascular Dynamics, Advanced Medical Engineering Center, National Cardiovascular Center Research Institute, 5-7-1 Fujishirodai, Suita, Osaka 565-8565, Japan (e-mail: torukawa@res.ncvc.go.jp).

The costs of publication of this article were defrayed in part by the payment of page charges. The article must therefore be hereby marked "*advertisement*" in accordance with 18 U.S.C. Section 1734 solely to indicate this fact.

the anterolateral free wall of the left ventricle perfused by the left anterior descending coronary artery (LAD) to monitor myocardial interstitial NE and ACh levels in the ischemic region during occlusion of the LAD (13). Another dialysis probe was implanted transversely into the posterior free wall of the left ventricle perfused by the left circumflex coronary artery to monitor myocardial interstitial NE and ACh levels in a nonischemic region. Heparin sodium (100 U/kg) was administered intravenously to prevent blood coagulation. Animals were divided into a normothermic group ($n = 8$) and a hypothermic group ($n = 6$). In the hypothermic group, surface cooling with ice bags was performed until the esophageal temperature decreased to 33°C (15, 16). A stable hypothermic condition was obtained within ~2 h. In each group, we occluded the LAD for 60 min and examined changes in the myocardial interstitial NE and ACh levels in the ischemic region (i.e., the LAD region) and nonischemic region (i.e., the left circumflex coronary artery region). Fifteen-minute dialysate samples were obtained during the preocclusion baseline condition and during the periods of 0–15, 15–30, 30–45, and 45–60 min of the LAD occlusion.

*Protocol 2: sympathetic stimulation.* We examined the effects of hypothermia on the sympathetic nerve stimulation-induced myocardial interstitial NE release ($n = 6$). A dialysis probe was implanted transversely into the anterolateral free wall of the left ventricle. The bilateral cardiac sympathetic nerves originating from the stellate ganglia were exposed through a second intercostal space and sectioned. The cardiac end of each sectioned nerve was placed on a bipolar platinum electrode for sympathetic stimulation (5 Hz, 10 V, 1-ms pulse duration). The electrodes and nerves were covered with mineral oil to provide insulation and prevent desiccation. A 4-min dialysate sample was obtained during the sympathetic stimulation under the normothermic condition. Thereafter, hypothermia was introduced using the same cooling procedure as in *protocol 1*, and a second 4-min dialysate sample was obtained during the sympathetic stimulation.

*Protocol 3: vagal stimulation.* We examined the effects of hypothermia on the vagal nerve stimulation-induced ACh release ($n = 5$). A dialysis probe was implanted transversely into the anterolateral free wall of the left ventricle. The bilateral vagi were exposed through a midline cervical incision and sectioned at the neck. The cardiac end of each sectioned nerve was placed on a bipolar platinum electrode for vagal stimulation (20 Hz, 10 V, 1-ms pulse duration). To prevent severe bradycardia and cardiac arrest, which can be induced by the vagal stimulation, the heart was paced at 200 beats/min using pacing wires attached to the apex of the heart during the stimulation period. A 4-min dialysate sample was obtained during the vagal stimulation under the normothermic condition. Thereafter, hypothermia was introduced using the same cooling procedure as in *protocol 1*, and a second 4-min dialysate sample was obtained during the vagal stimulation.

Because of the relatively intense stimulation of the sympathetic or vagal nerve, the stimulation period in *protocols 2* and *3* was limited to 4 min to minimize gradual waning of the stimulation effects. At the end of the experiment, the animals were killed by increasing the depth of anesthesia with an overdose of pentobarbital sodium. We then confirmed that the dialysis probes had been threaded in the middle layer of the left ventricular myocardium.

### *Dialysis Technique*

The dialysate NE and ACh concentrations were measured as indexes of myocardial interstitial NE and ACh levels, respectively. The materials and properties of the dialysis probe have been described previously (2, 3). Briefly, we designed a transverse dialysis probe. A dialysis fiber (13-mm length, 310-μm outer diameter, 200-μm inner diameter; PAN-1200, 50,000 molecular weight cutoff; Asahi Chemical) was connected at both ends to polyethylene tubes (25-cm length, 500-μm outer diameter, 200-μm inner diameter). The dialysis probe was perfused with Ringer solution containing a cholinesterase inhibitor eserine ($10^{-4}$ M) at a rate of 2 μl/min. We started dialysate sampling from 2 h after the implantation of the dialysis probe(s), when the dialysate NE and ACh concentrations had reached steady states. The actual dialysate sampling was delayed by 5 min from the collection period to account for the dead space volume between the semipermeable membrane and the sample tube. Each sample was collected in a microtube containing 3 μl of HCl to prevent amine oxidation. The dialysate ACh concentration was measured directly by HPLC with electrochemical detection (Eicom). The in vitro recovery rate of ACh was ~70%. With the use of a criterion of signal-to-noise ratio of higher than three, the detection limit for ACh was 3 pg per injection. The dialysate NE concentration was measured by another HPLC-electrochemical detection system after the removal of interfering compounds by an alumina procedure. The in vitro recovery rate of NE was ~55%. With the use of a criterion of signal-to-noise ratio of higher than three, the detection limit for NE was 200 fg per injection.

### *Statistical Analysis*

All data are presented as means and SD values. For *protocol 1*, we performed two-way repeated-measures ANOVA using hypothermia as one factor and the dialysate sampling periods (the effects of ischemia) as the other factor. For *protocols 2* and *3*, we compared stimulation-induced releases of NE and ACh before and during hypothermia using a paired *t*-test. For all of the statistics, the difference was considered significant when $P < 0.05$.

## RESULTS

Figure 1*A* illustrates changes in myocardial interstitial NE levels in the ischemic region during LAD occlusion obtained from *protocol 1*. The *inset* shows the magnified ordinate for the

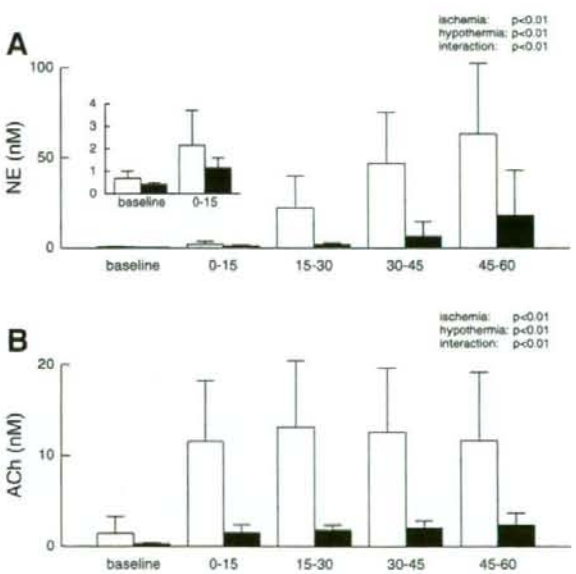


Fig. 1. *A*: ischemia-induced myocardial interstitial norepinephrine (NE) release in the ischemic region. Acute myocardial ischemia caused a progressive increase in the level of myocardial interstitial NE. Hypothermia attenuated the ischemia-induced NE release. *Inset*: magnified ordinate for the baseline and the 0- to 15-min period of ischemia. *B*: ischemia-induced myocardial interstitial ACh release in the ischemic region. Acute myocardial ischemia increased the myocardial interstitial ACh levels. Hypothermia attenuated the ischemia-induced ACh release. Open bars: normothermia; solid bars: hypothermia.

baseline and the 0- to 15-min period of ischemia. In the normothermic group (open bars), the LAD occlusion caused an ~94-fold increase in the NE level during the 45- to 60-min interval. In the hypothermic group (solid bars), the LAD occlusion caused an ~45-fold increase in the NE level during the 45- to 60-min interval. Compared with normothermia, hypothermia suppressed the baseline NE level to ~59% and the NE level during the 45- to 60-min period to ~29%. Statistical analysis indicated that the effects of both hypothermia and ischemia on the NE release were significant, and the interaction between hypothermia and ischemia was also significant.

Figure 1*B* illustrates changes in myocardial interstitial ACh levels in the ischemic region during the LAD occlusion. In both the normothermic (open bars) and hypothermic (solid bars) groups, the LAD occlusion caused an approximately eightfold increase in the ACh level during the 45- to 60-min interval. Compared with normothermia, however, hypothermia suppressed both the baseline ACh level and the ACh level during the 45- to 60-min period of ischemia to ~20%. Statistical analysis indicated that the effects of both hypothermia and ischemia on the ACh release were significant, and the interaction between hypothermia and ischemia was also significant.

Figure 2*A* illustrates changes in myocardial interstitial NE levels in the nonischemic region during the LAD occlusion. Note that scale of the ordinate is only one-hundredth of that in Fig. 1*A*. The LAD occlusion decreased the NE level in the normothermic group (open bars); the NE level during the 45- to 60-min interval was ~59% of the baseline level. The LAD occlusion also decreased the NE level in the hypothermic group (solid bars); the NE level during the 45- to 60-min interval was ~64% of the baseline level. Although the LAD occlusion resulted in a decrease in the NE level under both conditions, the NE level under hypothermia was nearly twice that measured under normothermia. The statistical analysis indicated that the effects of both hypothermia and ischemia on the NE release were significant, whereas the interaction between hypothermia and ischemia was not significant.

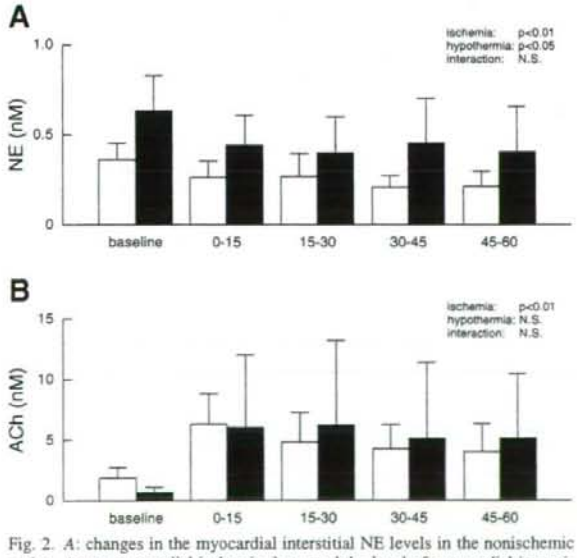


Fig. 2. *A*: changes in the myocardial interstitial NE levels in the nonischemic region. Acute myocardial ischemia decreased the level of myocardial interstitial NE from the baseline level. Hypothermia increased the myocardial interstitial NE levels in the nonischemic region. *B*: changes in the myocardial interstitial ACh levels in the nonischemic region. Acute myocardial ischemia increased the myocardial interstitial ACh level. Hypothermia did not attenuate the increasing response of ACh to the left anterior descending coronary artery occlusion. Open bars: normothermia; solid bars: hypothermia. NS, not significant.

Table 1. *Mean arterial pressure during acute myocardial ischemia obtained in protocol 1*

| | Baseline | 5 min | 15 min | 30 min | 45 min | 60 min |
|---|---|---|---|---|---|---|
| Normothermia | 108 (23) | 102 (28) | 101 (24) | 101 (20) | 102 (21) | 102 (21) |
| Hypothermia | 108 (11) | 80 (17) | 87 (10) | 85 (10) | 86 (10) | 91 (11) |

Values are means (SD) (in mmHg) obtained during preocclusion baseline period and 5-, 15-, 30-, 45-, and 60-min periods of coronary artery occlusion. Ischemia: $P < 0.01$; hypothermia: not significant; interaction: $P < 0.01$.

Figure 2*B* illustrates changes in myocardial interstitial ACh levels in the nonischemic region during the LAD occlusion. The LAD occlusion caused an ~3.4-fold increase in the ACh level during the 0- to 15-min interval in the normothermic group (open bars). The LAD occlusion caused an approximately ninefold increase in the ACh level during the 0- to 15-min interval in the hypothermic group (solid bars). These effects of ischemia on the ACh release were statistically significant. Although hypothermia seemed to attenuate the baseline ACh level, the overall effects of hypothermia on the ACh level were insignificant.

Tables 1 and 2 summarize the MAP and HR data, respectively, obtained in *protocol 1*. Acute myocardial ischemia significantly reduced MAP ($P < 0.01$) and HR ($P < 0.01$). Hypothermia did not affect MAP but did decrease HR ($P < 0.01$). The interaction between ischemia and hypothermia was significant for MAP but not for HR by the two-way repeated-measures ANOVA.

For *protocol 2*, hypothermia significantly attenuated the sympathetic stimulation-induced NE release to ~70% of the level observed during normothermia (Fig. 3*A*). Under normothermia, the sympathetic stimulation increased MAP from 114 mmHg (SD 27) to 134 mmHg (SD 33) ($P < 0.01$) and HR from 147 beats/min (SD 9) to 207 beats/min (SD 5) ($P < 0.01$). Under hypothermia, the sympathetic stimulation increased MAP from 117 mmHg (SD 11) to 136 mmHg (SD 22) ($P < 0.05$) and HR from 125 beats/min (SD 16) to 164 beats/min (SD 10) ($P < 0.01$).

For *protocol 3*, hypothermia significantly attenuated the vagal stimulation-induced ACh release to ~70% of the level observed during normothermia (Fig. 3*B*). Hypothermia did not change MAP [117 mmHg (SD 18) vs. 118 mmHg (SD 27)] but

Table 2. *Heart rate during acute myocardial ischemia obtained in protocol 1*

| | Baseline | 5 min | 15 min | 30 min | 45 min | 60 min |
|---|---|---|---|---|---|---|
| Normothermia | 183 (26) | 160 (18) | 163 (16) | 163 (18) | 166 (20) | 165 (21) |
| Hypothermia | 146 (25) | 116 (19) | 113 (19) | 126 (39) | 112 (20) | 97 (31) |

Values are means (SD) (in beats/min) obtained during preocclusion baseline period and 5-, 15-, 30-, 45-, and 60-min periods of coronary artery occlusion. Ischemia: $P < 0.01$; hypothermia: $P < 0.01$; interaction: not significant.

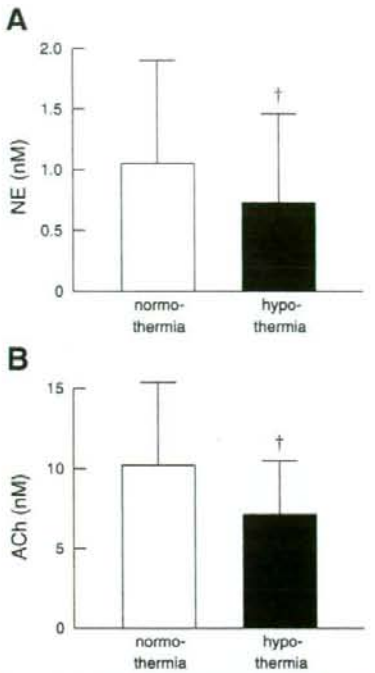


Fig. 3. *A*: efferent sympathetic nerve stimulation-induced release of myocardial interstitial NE before and during hypothermia. †Hypothermia significantly attenuated the stimulation-induced NE release. *B*: efferent vagal nerve stimulation-induced release of myocardial interstitial ACh before and during hypothermia. †Hypothermia significantly attenuated the stimulation-induced ACh release.

did decrease HR from 202 beats/min (SD 24) to 179 beats/min (SD 15) ($P < 0.05$) during the prestimulation, unpaced condition. MAP during the stimulation was 105 mmHg (SD 19) under normothermia and 93 mmHg (SD 33) under hypothermia.

## DISCUSSION

A cardiac microdialysis is a powerful tool to estimate neurotransmitter levels in the myocardial interstitium in vivo (2, 3, 14, 19, 20, 31). The present study demonstrated that hypothermia significantly attenuated the myocardial interstitial releases of NE and ACh in the ischemic region during the LAD occlusion. In contrast, the increasing response in the ACh level from its baseline level and the decreasing response in the NE level from its baseline level observed in the nonischemic region were maintained under hypothermia. To our knowledge, this is the first report showing the effects of hypothermia on the myocardial interstitial releases of NE and ACh during acute myocardial ischemia in vivo. In addition, the present study showed that hypothermia significantly attenuated nerve stimulation-induced myocardial interstitial NE and ACh releases in vivo.

### *Effects of Hypothermia on Ischemia-induced NE and ACh Releases in the Ischemic Region*

Acute myocardial ischemia causes energy depletion, which leads to myocardial interstitial NE release in the ischemic region (Fig. 1*A*). The NE release can be classified as exocytotic or nonexocytotic (18, 24). Exocytotic release indicates NE release from synaptic vesicles, which normally occurs in response to nerve discharge and subsequent $Ca^{2+}$ influx through voltage-dependent $Ca^{2+}$ channels. On the other hand, nonexocytotic release indicates NE release from the axoplasm, such as that mediated by a reverse transport through the NE transporter. A neuronal uptake blocker, desipramine, can suppress the ischemia-induced NE release (19, 24). Whereas exocytotic release contributes to the ischemia-induced NE release in the initial phase of ischemia (within ~20 min), carrier-mediated nonexocytotic release becomes predominant as the ischemic period is prolonged (1). Hypothermia significantly attenuated the ischemia-induced NE release (Fig. 1*A*). The NE level during the 45- to 60-min period of ischemia under hypothermia was ~20% of that obtained under normothermia. The NE uptake transporter is driven by the $Na^+$ gradient across the cell membrane (23). The loss of the $Na^+$ gradient due to ischemia causes NE to be transported out of the cell by reversing the action of the NE transporter. Hypothermia inhibits the action of the NE transporter and also suppresses the intracellular $Na^+$ accumulation (8), thereby reducing nonexocytotic NE release during ischemia. The present results are in line with an in vitro study that showed hypothermia suppressed nonexocytotic NE release induced by deprivation of oxygen and glucose (30). The present results are also consistent with a previous study from our laboratory that showed hypothermia attenuated the nonexocytotic NE release induced by ouabain, tyramine, or cyanide (16).

Acute myocardial ischemia increases myocardial interstitial ACh level in the ischemic region, as reported previously (Fig. 1*B*) (13). The level of ischemia-induced ACh release during 0- to 15-, 15- to 30-, 30- to 45-, or 45- to 60-min period of ischemia is comparable to that evoked by 4-min electrical stimulation of the bilateral vagi (Fig. 3*B*). Compared with the normothermic condition, hypothermia significantly attenuated the ischemia-induced myocardial interstitial release of ACh in the ischemic region. Our laboratory's previous study indicated that intracellular $Ca^{2+}$ mobilization is essential for the ischemia-induced release of ACh (13). Hypothermia may have prevented the $Ca^{2+}$ overload, thereby reducing the ischemia-induced ACh release. Alternatively, hypothermia may reduce the extent of the ischemic injury, which in turn suppressed the ischemia-induced ACh release. Because ACh has protective effects on the cardiomyocytes against ischemia (11), the suppression of ischemia-induced ACh release during hypothermia itself may be unfavorable for cardioprotection.

There is considerable controversy regarding the cardioprotective effects of β-adrenergic blockade during severe ischemia, with studies demonstrating a reduction of infarct size (10, 17) or no effects (7, 27). The β-adrenergic blockade seems effective to protect the heart only when the heart is reperfused within a certain period after the coronary occlusion. The β-adrenergic blockade would reduce the myocardial oxygen consumption through the reduction of HR and ventricular contractility and delay the progression of ischemic injury. Hence the infarct size might be reduced when the heart is reperfused before the ischemic damage becomes irreversible. The ischemia-induced NE release reached nearly 100 times the baseline NE level under normothermia (Fig. 1*A*), which by far exceeded the NE level attained by electrical stimulation of the

bilateral stellate ganglia (Fig. 3A). Because high NE levels have cardiotoxic effects (22), ischemia-induced NE release might aggravate the ischemic injury. However, catecholamine depletion by a reserpine treatment fails to reduce the infarct size (26, 29), throwing a doubt on the involvement of catecholamine toxicity in the progression of myocardial damage during ischemia. It is, therefore, most likely that the hypothermia-induced reductions in NE and ACh are the result of reduced myocardial damage or a direct effect on nerve endings.

Van den Doel et al. (28) showed that hypothermia does not abolish necrosis, but rather delays necrosis during sustained ischemia, so that hypothermia protected against infarction produced by a 30-min occlusion but not against infarction produced by a 60-min occlusion in the rat heart. At the same time, they mentioned that hypothermia was able to reduce the infarct size after a 60-min coronary occlusion in the dog, possibly because of the significant collateral flow in the canine hearts. Because the feline hearts are similar to the canine hearts in that they have considerable collateral flow compared with the rat hearts (21), hypothermia should have protected the feline heart against the 60-min coronary occlusion in the present study.

*Effects of Hypothermia on the NE and ACh Releases in the Nonischemic Region and on the Electrical Stimulation-induced NE and ACh Releases*

The NE and ACh levels in the nonischemic region may reflect the sympathetic and parasympathetic drives to this region. As an example, myocardial interstitial ACh levels increase during activations of the arterial baroreflex and the Bezold-Jarisch reflex (14). In the present study, acute myocardial ischemia decreased the NE level from its baseline level, whereas it increased the ACh level from its baseline level (Fig. 2). Ischemia also decreased MAP and HR (Tables 1 and 2), suggesting that the Bezold-Jarisch reflex was induced by the LAD occlusion under both normothermia and hypothermia. Taking into account the fact that electrical stimulation-induced ACh release was attenuated to ~70% (Fig. 3), similar ACh levels during ischemia imply the enhancement of the parasympathetic outflow via the Bezold-Jarisch reflex under hypothermia. These results are in line with the study by Zheng et al. (32), where pulmonary chemoreflex-induced bradycardia was maintained under hypothermia. Hypothermia increased the NE level in the nonischemic region, suggesting that sympathetic drive to this region also increased. Hypothermic stress is known to cause sympathetic activation, accompanying increases in MAP, HR, plasma NE, and epinephrine levels (4). In the present study, because the effect of hypothermia on MAP was insignificant (Table 1) and HR decreased under hypothermia (Table 2), the sympathetic activation observed in the nonischemic region might have been regional and not systemic.

Hypothermia attenuated the releases of NE and ACh in response to respective nerve stimulation to ~70% of that observed under normothermia (Fig. 3). The suppression of the exocytotic NE release by hypothermia is consistent with a previous study from our laboratory, where hypothermia attenuated the myocardial interstitial NE release in response to vena cava occlusion or to a local high $K^+$ administration (15). The suppression of NE release by hypothermia is consistent with an in vitro study by Kao and Westhead (12) in which catecholamine secretion from adrenal chromaffin cells induced by elevated $K^+$ levels increased as the temperature increased from 4 to 37°C. On the other hand, because hypothermia inhibits the neuronal NE uptake, the NE concentration at the synaptic cleft is expected to be increased if the level of NE release remains unchanged. Actually, Vizi (30) demonstrated that hypothermia increased NE release in response to field stimulation in vitro. In the present study, however, the suppression of NE release might have canceled the potential accumulation of NE due to NE uptake inhibition. The present study also demonstrated that the ACh release was suppressed by hypothermia. In the rat striatum, hypothermia decreases the extracellular ACh concentration and increases the choline concentration (5). Hypothermia may inhibit a choline uptake transporter in the same manner as it inhibits a NE uptake transporter. The inhibition of the choline transporter by hypothermia may have hampered the replenishment of the available pool of ACh and thereby contributed to the suppression of the stimulation-induced ACh release.

*Limitations*

In *protocol 1*, because we did not measure the infarct size in the present study, the degree of myocardial protection by hypothermia was undetermined. Whether the reduction of ischemia-induced neurotransmitter release correlates with the reduction of infact size requires further investigations. In *protocols 2* and *3*, baseline NE and ACh levels were not measured. The reduction of stimulation-induced NE and ACh release by hypothermia might be partly due to the reduction of baseline NE and ACh levels. However, because transection of the stellate ganglia (31) or vagi (3) reduces the baseline NE and ACh levels, changes in the baseline NE and ACh levels by hypothermia in *protocols 2* and *3* could not be as large as those observed under innervated conditions in *protocol 1* (Figs. 1 and 2).

In conclusion, hypothermia attenuated the ischemia-induced releases of NE and ACh in the ischemic region to ~30 and 20% of those observed under normothermia, respectively. Hypothermia also attenuated the nerve stimulation-induced releases of NE and ACh to ~70% of those observed during normothermia. In contrast, hypothermia did not affect the decreasing response in the NE level and the increasing response in the ACh level in the nonischemic region, suggesting that the Bezold-Jarisch reflex evoked by the LAD occlusion was maintained.

**GRANTS**

This study was supported by Health and Labour Sciences Research Grant for Research on Advanced Medical Technology, Health and Labour Sciences Research Grant for Research on Medical Devices for Analyzing, Supporting and Substituting the Function of Human Body, and Health and Labour Sciences Research Grant H18-Iryo-Ippan-023 from the Ministry of Health, Labour and Welfare of Japan; Program for Promotion of Fundamental Studies in Health Science from the National Institute of Biomedical Innovation; a grant provided by the Ichiro Kanehara Foundation; Ground-based Research Announcement for Space Utilization promoted by the Japan Space Forum; and Industrial Technology Research Grant Program 03A47075 from the New Energy and Industrial Technology Development Organization of Japan.

**REFERENCES**

1. **Akiyama T, Yamazaki T.** Norepinephrine release from cardiac sympathetic nerve endings in the in vivo ischemic region. *J Cardiovasc Pharmacol* 34: S11–S14, 1999.

2. **Akiyama T, Yamazaki T, Ninomiya I.** In vivo monitoring of myocardial interstitial norepinephrine by dialysis technique. *Am J Physiol Heart Circ Physiol* 261: H1643–H1647, 1991.
3. **Akiyama T, Yamazaki T, Ninomiya I.** In vivo detection of endogenous acetylcholine release in cat ventricles. *Am J Physiol Heart Circ Physiol* 266: H854–H860, 1994.
4. **Chernow B, Lake CR, Zaritsky A, Finton CK, Casey L, Rainey TG, Fletcher JR.** Sympathetic nervous system "switch off" with severe hypothermia. *Crit Care Med* 11: 677–680, 1983.
5. **Damsma G, Fibiger HC.** The effects of anaesthesia and hypothermia on interstitial concentrations of acetylcholine and choline in rat striatum. *Life Sci* 48: 2469–2474, 1991.
6. **Duncker DJ, Klassen CL, Ishibashi Y, Herrlinger SH, Pavek T, Bache R.** Effect of temperature on myocardial infarction in swine. *Am J Physiol Heart Circ Physiol* 270: H1189–H1199, 1996.
7. **Genth K, Hofmann M, Hofmann M, Schaper W.** The effect of β-adrenergic blockade on infarct size following experimental coronary occlusion. *Basic Res Cardiol* 76: 144–151, 1981.
8. **Gerevich Z, Tretter L, Adam-Vizi V, Baranyi M, Kiss JP, Zelles T, Vizi ES.** Analysis of high intracellular [$Na^+$]-induced release of [$^3$H]noradrenaline in rat hippocampal slices. *Neuroscience* 104: 761–768, 2001.
9. **Hale SL, Kloner RA.** Myocardial temperature in acute myocardial infarction: protection with mild regional hypothermia. *Am J Physiol Heart Circ Physiol* 273: H220–H227, 1997.
10. **Jang IK, Van de Werf F, Vanhaecke J, De Geest H.** Coronary reperfusion by thrombolysis and early beta-adrenergic blockade in acute experimental myocardial infarction. *J Am Coll Cardiol* 14: 1816–1823, 1989.
11. **Kakinuma Y, Ando M, Kuwabara M, Katare RG, Okudela K, Kobayashi M, Sato T.** Acetylcholine from vagal stimulation protects cardiomyocytes against ischemia and hypoxia involving additive nonhypoxic induction of HIF-1α. *FEBS Lett* 579: 2111–2118, 2005.
12. **Kao LS, Westhead EW.** Temperature dependence of catecholamine secretion from cultured bovine chromaffin cells. *J Neurochem* 43: 590–592, 1984.
13. **Kawada T, Yamazaki T, Akiyama T, Sato T, Shishido T, Inagaki M, Takaki H, Sugimachi M, Sunagawa K.** Differential acetylcholine release mechanisms in the ischemic and non-ischemic myocardium. *J Mol Cell Cardiol* 32: 405–414, 2000.
14. **Kawada T, Yamazaki T, Akiyama T, Shishido T, Inagaki M, Uemura K, Miyamoto T, Sugimachi M, Takaki H, Sunagawa K.** In vivo assessment of acetylcholine-releasing function at cardiac vagal nerve terminals. *Am J Physiol Heart Circ Physiol* 281: H139–H145, 2001.
15. **Kitagawa H, Akiyama T, Yamazaki T.** Effects of moderate hypothermia on in situ cardiac sympathetic nerve endings. *Neurochem Int* 40: 235–242, 2002.
16. **Kitagawa H, Yamazaki T, Akiyama T, Mori H, Sunagawa K.** Effects of moderate hypothermia on norepinephrine release evoked by ouabain, tyramine and cyanide. *J Cardiovasc Pharmacol* 41: S111–S114, 2003.
17. **Ku DD, Lucchesi BR.** Effects of dimethyl propranolol (UM-272; SC-27761) on myocardial ischemic injury in the canine heart after temporary coronary artery occlusion. *Circulation* 57: 541–548, 1978.
18. **Kurz T, Richardt G, Hagl S, Seyfarth M, Schömig A.** Two different mechanisms of noradrenaline release during normoxia and simulated ischemia in human cardiac tissue. *J Mol Cell Cardiol* 27: 1161–1172, 1995.
19. **Lameris TW, de Zeeuw S, Alberts G, Boomsma F, Duncker DJ, Verdouw PD, Veld AJ, van den Meiracker AH.** Time course and mechanism of myocardial catecholamine release during transient ischemia in vivo. *Circulation* 101: 2645–2650, 2000.
20. **Lameris TW, de Zeeuw S, Duncker DJ, Alberts G, Boomsma F, Verdouw PD, van den Meiracker AH.** Exogenous angiotensin II does not facilitate norepinephrine release in the heart. *Hypertension* 40: 491–497, 2002.
21. **Maxwell MP, Hearse DJ, Yellon DM.** Species variation in the coronary collateral circulation during regional myocardial ischaemia: a critical determinant of the rate of evolution and extent of myocardial infarction. *Cardiovasc Res* 21: 737–746, 1987.
22. **Rona G.** Catecholamine cardiotoxicity. *J Mol Cell Cardiol* 17: 291–306, 1985.
23. **Schwartz JH.** Neurotransmitters. In: *Principles of Neural Science* (4th Ed.), edited by Kandel ER, Schwartz JH, Jessell TM. New York: McGraw-Hill, 2000, p. 280–297.
24. **Schömig A, Kurz T, Richardt G, Schömig E.** Neuronal sodium homeostasis and axoplasmic amine concentration determine calcium-independent noradrenaline release in normoxic and ischemic rat heart. *Circ Res* 63: 214–226, 1988.
25. **Simkhovich BZ, Hale SL, Kloner RA.** Metabolic mechanism by which mild regional hypothermia preserves ischemic tissue. *J Cardiovasc Pharmacol Ther* 9: 83–90, 2004.
26. **Toombs CF, Wiltse AL, Shebuski RJ.** Ischemic preconditioning fails to limit infarct size in reserpinized rabbit myocardium. Implication of norepinephrine release in the preconditioning effect. *Circulation* 88: 2351–2358, 1993.
27. **Torr S, Drake-Holland AJ, Main M, Hynd J, Isted K, Noble MIM.** Effects on infarct size of reperfusion and pretreatment with β-blockade and calcium antagonists. *Basic Res Cardiol* 84: 564–582, 1989.
28. **Van den Doel MA, Gho BC, Duval SY, Schoemaker RG, Duncker DJ, Verdouw PD.** Hypothermia extends the cardioprotection by ischaemic preconditioning to coronary artery occlusions of longer duration. *Cardiovasc Res* 37: 76–81, 1998.
29. **Vander Heide RS, Schwartz LM, Jennings RB, Reimer KA.** Effect of catecholamine depletion on myocardial infarct size in dogs: role of catecholamines in ischemic preconditioning. *Cardiovasc Res* 30: 656–662, 1995.
30. **Vizi ES.** Different temperature dependence of carrier-mediated (cytoplasmic) and stimulus-evoked (exocytotic) release of transmitter: a simple method to separate the two types of release. *Neurochem Int* 33: 359–366, 1998.
31. **Yamazaki T, Akiyama T, Kitagawa H, Takauchi Y, Kawada T, Sunagawa K.** A new, concise dialysis approach to assessment of cardiac sympathetic nerve terminal abnormalities. *Am J Physiol Heart Circ Physiol* 272: H1182–H1187, 1997.
32. **Zheng F, Kidd C, Bowser-Riley F.** Effects of moderate hypothermia on baroreflex and pulmonary chemoreflex heart rate response in decerebrate ferrets. *Exp Physiol* 81: 409–420, 1996.

*Am J Physiol Heart Circ Physiol* 293: H2254–H2261, 2007.
First published August 10, 2007; doi:10.1152/ajpheart.00490.2007.

# Efferent vagal nerve stimulation induces tissue inhibitor of metalloproteinase-1 in myocardial ischemia-reperfusion injury in rabbit

**Kazunori Uemura,[1] Meihua Li,[1] Takaki Tsutsumi,[2] Toji Yamazaki,[3] Toru Kawada,[1] Atsunori Kamiya,[1] Masashi Inagaki,[1] Kenji Sunagawa,[2] and Masaru Sugimachi[1]**

*Departments of [1]Cardiovascular Dynamics and [3]Cardiac Physiology, National Cardiovascular Center Research Institute, Suita, Japan; and [2]Department of Cardiovascular Medicine, Kyushu University Graduate School of Medical Science, Fukuoka, Japan*

Submitted 24 April 2007; accepted in final form 7 August 2007

**Uemura K, Li M, Tsutsumi T, Yamazaki T, Kawada T, Kamiya A, Inagaki M, Sunagawa K, Sugimachi M.** Efferent vagal nerve stimulation induces tissue inhibitor of metalloproteinase-1 in myocardial ischemia-reperfusion injury in rabbit. *Am J Physiol Heart Circ Physiol* 293: H2254–H2261, 2007. First published August 10, 2007; doi:10.1152/ajpheart.00490.2007.—Vagal nerve stimulation has been suggested to ameliorate left ventricular (LV) remodeling in heart failure. However, it is not known whether and to what degree vagal nerve stimulation affects matrix metalloproteinase (MMP) and tissue inhibitor of MMP (TIMP) in myocardium, which are known to play crucial roles in LV remodeling. We therefore investigated the effects of electrical stimulation of efferent vagal nerve on myocardial expression and activation of MMPs and TIMPs in a rabbit model of myocardial ischemia-reperfusion (I/R) injury. Anesthetized rabbits were subjected to 60 min of left coronary artery occlusion and 180 min of reperfusion with (I/R-VS, $n = 8$) or without vagal nerve stimulation (I/R, $n = 7$). Rabbits not subjected to coronary occlusion with (VS, $n = 7$) or without vagal stimulation (sham, $n = 7$) were used as controls. Total MMP-9 protein increased significantly after left coronary artery occlusion in I/R-VS and I/R to a similar degree compared with VS and sham values. Endogenous active MMP-9 protein level was significantly lower in I/R-VS compared with I/R. TIMP-1 mRNA expression was significantly increased in I/R-VS compared with the I/R, VS, and sham groups. TIMP-1 protein was significantly increased in I/R-VS and VS compared with the I/R and sham groups. Cardiac microdialysis technique demonstrated that topical perfusion of acetylcholine increased dialysate TIMP-1 protein level, which was suppressed by coperfusion of atropine. Immunohistochemistry demonstrated a strong expression of TIMP-1 protein in cardiomyocytes around the dialysis probe used to perfuse acetylcholine. In conclusion, in a rabbit model of myocardial I/R injury, vagal nerve stimulation induced TIMP-1 expression in cardiomyocytes and reduced active MMP-9.

myocardial remodeling; matrix metalloproteinase; acetylcholine

LEFT VENTRICULAR (LV) myocardial remodeling that occurs after myocardial infarction (MI) leads to progressive LV dilation and eventually pump dysfunction (33, 40). In addition to the loss of contractile cardiomyocytes, pathological degradation and reconstitution of extracellular matrix significantly contribute to the progression of LV remodeling, where matrix metalloproteinase (MMP) and its intrinsic inhibitor, tissue inhibitor of MMP (TIMP), play crucial roles (37, 43).

A previous study using genetically engineered mice demonstrated that target deletion of the MMP-9 gene prevented LV rupture and ameliorated LV remodeling after MI (10). The positive results of MMP inhibition on LV remodeling in animal models led to the proposal to use MMP inhibitors as a potential therapy for patients at risk for the development of heart failure after MI (27, 32). However, recent clinical results from the Prevention of Myocardial Infarction Early Remodeling (PREMIER) trial failed to demonstrate a beneficial effect of MMP inhibition on LV remodeling after MI (16). This indicates the importance of further understanding the in vivo regulatory mechanisms of MMPs to understand and beneficially modify the LV remodeling process.

The cardiac autonomic nervous system plays an important role in the progression of heart failure (21). A previous communication from our laboratory demonstrated that chronic electrical stimulation of vagal nerve ameliorated LV remodeling and markedly improved survival after MI in rat (23). However, it is not known whether and to what degree the vagal nerve affects the MMPs and the TIMPs in vivo. We therefore investigated the effects of electrical stimulation of vagal nerve on myocardial expression of MMP-2/9 and TIMP-1/2 in a rabbit model of myocardial ischemia-reperfusion (I/R) injury. We also investigated the direct action of acetylcholine (ACh), a neurotransmitter released by vagal nerve stimulation (VNS), on myocardial release of TIMP-1 using a cardiac microdialysis technique (19). Our results indicated that VNS induced expression of TIMP-1 from cardiomyocytes and reduced active MMP-9 in myocardial I/R injury in rabbit.

## METHODS

We used 49 Japanese white rabbits in this study (male, 2.5–3.0 kg). Care of the animals was in strict accordance with the guiding principles of the Physiological Society of Japan. All protocols were approved by the Animal Subjects Committee of the National Cardiovascular Center.

### *I/R Study*

*Experimental preparation.* Anesthesia was induced by intravenous injection of pentobarbital sodium (35 mg/kg). Animals were tracheotomized, intubated, and mechanically ventilated. Arterial pH, $P_{O_2}$, and $P_{CO_2}$ were maintained within the physiological ranges by supplying oxygen and changing the respiratory rate. α-Chloralose (20 $mg \cdot kg^{-1} \cdot h^{-1}$) was continuously infused to maintain an appropriate level of anesthesia during the experiment. A catheter-tipped micromanometer (SPC-330A, Millar Instruments, Houston, TX) was inserted via the right femoral artery to measure arterial pressure (AP). After a median sternotomy, the heart was suspended in a pericardial

Address for reprint requests and other correspondence: K. Uemura, Dept. of Cardiovascular Dynamics, National Cardiovascular Center Research Inst., 5-7-1 Fujishirodai, Suita 565-8565, Japan (e-mail: kuemura@ri.ncvc.go.jp).

The costs of publication of this article were defrayed in part by the payment of page charges. The article must therefore be hereby marked "*advertisement*" in accordance with 18 U.S.C. Section 1734 solely to indicate this fact.

cradle. Another catheter-tipped micromanometer was introduced into the LV via the apex to measure LV pressure (LVP). Piezoelectric crystals (1 mm, Sonometrics, Ontario, Canada) were attached to the anterior and lateral walls of the LV using cyanoacrylate adhesive (3M, Vetbond, St. Paul, MN) to measure regional LV segmental length. A 4-0 proline suture was passed around the main branch of the left anterior descending coronary artery (LAD), and a snare was formed by passing the ends of the thread through a small vinyl tube. A surface electrocardiogram (ECG) was recorded.

Bilateral cervical vagi were identified and transected at the neck region. A pair of bipolar electrodes was attached at the cardiac end of the right vagal nerve. The duration of electrical pulse used to stimulate the vagal nerve was set at 4 ms. We adjusted the amplitude of the pulse in each animal to reduce heart rate (HR) by 30% from the baseline value at a stimulation frequency of 10 Hz. The resultant stimulation voltage was 2–4 V.

*Experimental protocol.* Thirty minutes were allowed for stabilization after the initial preparation and surgical procedures were completed. The animals were randomized into the following four groups: *1*) sham group ($n = 7$), in which surgical preparation was conducted without coronary occlusion or vagal stimulation (VS); *2*) VS group ($n = 7$), in which stimulation of the vagal nerve was started after baseline hemodynamics were obtained and continued during the experiment; *3*) I/R group ($n = 7$), in which 60 min of LAD occlusion and 180 min of reperfusion were conducted; and *4*) I/R-VS group ($n = 8$), in which stimulation of the vagal nerve was started 15 min before LAD occlusion and continued throughout 60 min of myocardial ischemia and 180 min of reperfusion.

Baseline hemodynamic data (baseline) were recorded in all groups. A second set of measurements of hemodynamic data (60 min) was obtained during the last 5 min of the 60-min observation period in the sham and VS groups or during the last 5 min of the 60-min ischemic period in the I/R and I/R-VS groups. A third set of measurements of hemodynamic data (240 min) was recorded during the last 5 min of the next 180-min observation period in the sham and VS groups or during the last 5 min of the 180-min reperfusion period in the I/R and I/R-VS groups.

At each time point, hemodynamic data were recorded under a steady-state condition. All data acquisitions were done at end expiration. Analog signals of AP, LVP, segmental length of the anterior-lateral wall of LV (risk area), and ECG were digitized at 200 Hz and stored in a computer for off-line analysis (Sonolab, Sonometrics).

At the end of the experiment, the animal was euthanized. The whole heart was quickly excised and washed with cold PBS. After the vasculature, right ventricular free wall, and atrial appendages were dissected away, the remaining LV wall was snap frozen in liquid nitrogen and stored at −80°C.

*Myocardial protein extraction.* Approximately 200 mg of myocardial tissue sample obtained from the center of the risk area (anterior wall) of the LV free wall was homogenized in 1 ml of lysis buffer containing 50 mmol/l Tris (pH 7.4), 1.5 mmol/l $CaCl_2$, and 0.5% Triton X-100. The homogenate was centrifuged at 2,000 *g* for 10 min at 4°C, and the supernatant was collected. Protein concentration of each supernatant sample was determined with a DC Protein assay kit (Bio-Rad, Richmond, CA).

*Gelatin zymography.* Gelatin zymography was performed to assess the relative contents of the gelatinases MMP-2 and MMP-9 (43). The supernatants (60 μg protein) were loaded in Novex precast 10% Tris-glycine gels containing 0.1% gelatin (Invitrogen, Carlsbad, CA) and then electrophoresed. After renaturation and equilibration, the gels were incubated for 30 h at 37°C in Novex zymogram-developing buffer. The gels were then stained in 0.5% Coomassie blue G-250, dissolved in 30% methanol-10% acetic acid for 60 min, and destained in several changes of methanol-acetic acid for 60 min. Gels were dried and scanned. MMP-2 and MMP-9 related bands were analyzed using the NIH Image software (ImageJ 1.37).

*MMP-9 activity assay.* Bioactivity assay for MMP-9 was performed using the Biotrak activity assay system (GE Healthcare Bio-Sciences, Piscataway, NJ) following the manufacturer's instructions (42). Briefly, supernatant samples were placed in microtitre well plates coated with anti-MMP-9 (100 μl/well). The plates were incubated overnight at 4°C. The following day, *p*-aminophenylmercuric acetate was added to the wells for measuring "total" MMP-9 (pro- and active MMP-9). Buffer alone was added to the wells for measuring "active" (endogenous active MMP-9) MMP-9. Detection agent was then added to all wells (50 μl/well), and the plate was read at 405 nm ($t = 0$ min) and again after a 2-h incubation at 37°C. The value of MMP-9 was standardized by the protein concentration. All measurements were run in duplicate.

*ELISA measurement of TIMP-1 and TIMP-2.* Commercially available ELISA kits (Daiichi Fine Chemical, Toyama, Japan) were used to measure TIMP-1 and TIMP-2 levels in supernatants according to the manufacturer's instructions (13, 17, 20). Briefly, standards and samples were incubated in microtitre wells coated with anti-TIMP-1 and anti-TIMP-2 antibody. Peroxidase-labeled antibodies directed to the respective TIMPs were added to the corresponding wells. Visualization of the presence of the peroxidase label was achieved using the *o*-phenylenediamine substrate (TIMP-1) or tetramethylbenzidine substrate (TIMP-2). The plates were read at 490 (TIMP-1) or 450 (TIMP-2) nm. Values of TIMPs were standardized by the protein concentration. Since the ELISA systems have some degree of intraplate and interplate variability (<15%) (7), all measurements were run in duplicate to quadruplicate.

*Myocardial RNA extraction and reverse transcription.* Total RNA was extracted from the risk area (anterior wall) of the LV free wall by an acid guanidium thiocyanate-phenol chloroform method (Isogen, Nippon Gene). First-strand cDNA was synthesized using reverse transcriptase with random hexamer primers from 1 μg of total RNA in a final volume of 20 μl, according to the manufacturer's protocol (ReverTra Ace, Toyobo).

*Real-time quantitative reverse transcription-PCR.* To analyze TIMP-1 gene expression in myocardial tissue, real-time polymerase chain reaction (PCR) amplification was performed with SYBR Premix Ex Taq (Perfect Real Time; TaKaRa, Japan) using the ABI PRISM 7500 sequence detection system (Applied Biosystems). For standardization and quantification, rabbit glyceraldehyde 3-phosphate dehydrogenase (GAPDH) was amplified simultaneously. The respective PCR primers were designed from GenBank databases (Table 1). The PCR consisted of initial treatments (50°C, 2 min; and 95°C, 10 min) followed by 40 three-step cycles (denaturation 94°C, 10 s; annealing 60°C, 10 s; and extension 72°C, 40 s). Fluorescence was detected at the end of every extension phase (72°C). After PCR amplification, dissociation curves were constructed to confirm the formation of the intended PCR products. Relative expression of TIMP-1 to the GAPDH levels was calculated as described previously (28, 45).

*Hemodynamic data analysis.* The following hemodynamic parameters were determined from hemodynamic data: HR, mean arterial pressure, maximum first derivative of LVP (LV $dP/dt_{max}$), and fractional shortening of anterior-lateral wall (FS). End diastole and end ejection were defined as the peak of R wave of ECG and the peak of minimum first derivative of LVP, respectively. FS was calculated as

Table 1. *Probes used for real-time PCR*

| Assay | Sequence | Accession Number |
|---|---|---|
| TIMP-1 | | |
| Forward | 5′-CAACTCCGACCTTGTCATCAG-3′ | AY829731 |
| Reverse | 5′-GCGTCAAATCCTTTGAACATCT-3′ | |
| GAPDH | | |
| Forward | 5′-GGAGAAAGCTGCTAAGTATGACG-3′ | L23961 |
| Reverse | 5′-CACTGTTGA AGTCGCAGGAG-3′ | |

TIMP-1, tissue inhibitor of matrix metalloproteinase-1.

the ratio of systolic stroke change in segmental length and end-diastolic length of the anterior-lateral wall (36).

*Cardiac Microdialysis Study*

*Experimental preparation.* Experimental preparation was the same as described above in *I/R Study*, except that no coronary artery occlusion was performed. A microdialysis probe was implanted into the LV anterior wall. Heparin sodium (200 U/kg) was administered intravenously to prevent blood coagulation (19).

*Dialysis technique.* The materials and properties of the dialysis probe have been described (19). Briefly, we designed a hand-made long transverse dialysis probe. One end of a polyethylene tube (25 cm long, 0.5 mm OD, and 0.2 mm ID) was dilated with a 27-gauge needle (0.4 mm OD). Each end of the dialysis fiber (8 mm long, 0.215 mm OD, 0.175 mm ID, and 300 Å pore size; Evaflux type 5A, Kuraray Medical, Tokyo, Japan) was inserted into the polyethylene tube and glued.

Recovery of TIMP-1 passing through the dialysis fiber membrane was evaluated in vitro. The dialysis probe ($n = 4$) was immersed in Ringer solution (in mM; 147.0 NaCl, 4.0 KCl, and 2.25 $CaCl_2$) containing Tween 20 (0.1%) and various concentrations of TIMP-1 (10–40 ng/ml, free form of human TIMP-1, Daiichi Fine Chemical). The dialysis probe was perfused with Ringer solution at a rate of 2.5 μl/min using a microinjection pump (model CMA/102, Carnegie Medicine). We measured the concentration of TIMP-1 in the dialysate sample using an ELISA kit. The relative recovery of TIMP-1 was calculated as the ratio of TIMP-1 concentration in dialysate to its concentration in the medium surrounding the probe (11, 22). The relative recovery of TIMP-1 was 11.1 ± 0.3%. Recovery was constant between probes and within the probe for the TIMP-1 concentration range studied.

A fine-guiding needle (25 mm long, 0.51 mm OD, and 0.25 mm ID) was used for implantation of the dialysis probes. The guiding needle was connected to the dialysis probe with a stainless steel rod (5 mm long and 0.25 mm OD). Experimental protocols were initiated 2 h after implanting the dialysis probe. The dialysate sampling period was set at 60 min and was performed taking into account the dead space volume between the dialysis membrane and the sample tube.

*Experimental protocol.* After baseline dialysate was sampled and baseline hemodynamic data were recorded, the animals were randomized into the following three groups: *1*) VNS group ($n = 5$), in which electrical stimulation of vagal nerve was performed while the LV wall was perfused with Ringer solution via the dialysis probe; *2*) ACh group ($n = 8$), in which the LV wall was perfused with Ringer solution containing ACh (1 mM); and *3*) ACh-atropine (Atr) group ($n = 7$), in which the LV wall was perfused with Ringer solution containing ACh (1 mM) and Atr (0.2 mM). At 150 min after randomization, dialysate sampling and hemodynamic data recording were performed.

At the end of the experiment, the animal was euthanized. From selected hearts, transmural blocks of the LV free wall containing the dialysis probe were fixed in 4% paraformaldehyde for immunohistochemistry.

*Immunohistochemistry and confocal microscopy.* To investigate the distribution of TIMP-1, we performed confocal image analysis of LV tissue stained with anti-TIMP-1 antibody. Fixed blocks of LV tissues were washed in 0.1 mol/l phosphate buffer (pH 7.4), embedded in paraffin, and sectioned at a thickness of 5 μm. Sections were deparaffinized using xylene, rehydrated with serial grades of ethanol, and followed by hydration with distilled water. For antigen retrieval of TIMP-1 protein, specimens were immersed in a vessel filled with Target Retrieval Solution (pH 6.1; DAKO). The vessel containing the specimens was autoclaved at 121°C for 20 min. The slides were then allowed to cool at room temperature for 20 min to complete antigen unmasking. The sections were then incubated for 30 h with a mouse anti-TIMP-1 antibody (7-6C1, Daiichi Fine Chemical) diluted 1:5 and then incubated for 2 h in Alexa-488-conjugated goat anti-mouse Ig-G (Molecular Probes) diluted 1:200. Fluorescence of Alexa-488 was observed with a confocal laser-scanning microscope system (FV 300, Olympus). Reconstructed projection images were obtained from serial optical sections recorded at an interval of 0.5 μm.

*Exclusion Criteria*

Animals were excluded from the study when the following criteria were met: *1*) in the I/R study, coronary artery occlusion did not produce substantial regional dysfunction (FS of the risk area after occlusion was not <20% of the baseline value); *2*) intractable ventricular fibrillation or atrial tachycardia occurred; and *3*) the animal died during the surgical procedure, and the protocol was not completed.

*Statistical Analysis*

All data are presented as means ± SE. Tukey-Welsch's step-down multiple comparison test was used to determine the significance of differences among groups. $P$ values <0.05 were considered statistically significant.

## RESULTS

*I/R Study*

As shown in Fig. 1*A*, zymography of the myocardial extracts detected two bands at 92 and 72 kDa, corresponding to MMP-9 and MMP-2, respectively. Densitometric analysis demonstrated that relative MMP-9 level increased to a similar degree in the I/R and I/R-VS groups compared with the sham and VS groups (Fig. 1*B*). The relative MMP-2 level decreased in the I/R group compared with the sham and I/R-VS groups (Fig. 1*C*).

Bioactivity assays demonstrated that myocardial levels of total MMP-9 protein increased to a similar degree in the I/R and I/R-VS groups compared with sham and VS groups (Fig. 2*A*). Levels of endogenous active MMP-9 protein also increased in the I/R and I/R-VS groups compared with the sham and VS groups (Fig. 2*B*). The level of active MMP-9 in the I/R-VS group was significantly lower than that in the I/R group (<50%, $P < 0.01$).

The myocardial level of TIMP-1 protein increased in the VS and I/R-VS groups compared with the sham and I/R groups (Fig. 3*A*). There was no significant difference in the myocardial level of TIMP-2 protein among the four groups (Fig. 3*B*). TIMP-1 mRNA as measured by real-time RT-PCR was increased in the I/R-VS group compared with the sham, VS, and I/R groups (Fig. 3*C*).

Table 2 summarizes the data of systemic hemodynamics and LV function during the I/R study. In the VS and I/R-VS groups, HR decreased significantly compared with sham and I/R values at 60 and 240 min. In the I/R and I/R-VS groups, FS was depressed during ischemia with only partial recovery after reperfusion. In the I/R and I/R-VS groups, sonomicrometry demonstrated early systolic bulging of the anterior LV wall during ischemia as reflected by negative FS at the 60-min time point. There was no significant difference in LV $dP/dt_{max}$ and FS between the I/R and I/R-VS groups at 60 and 240 min.

*Cardiac Microdialysis Study*

Figure 4 presents dialysate TIMP-1 concentrations in response to electrical stimulation of the vagal nerve, to perfusion of ACh, and to perfusion of ACh with Atr. There were no

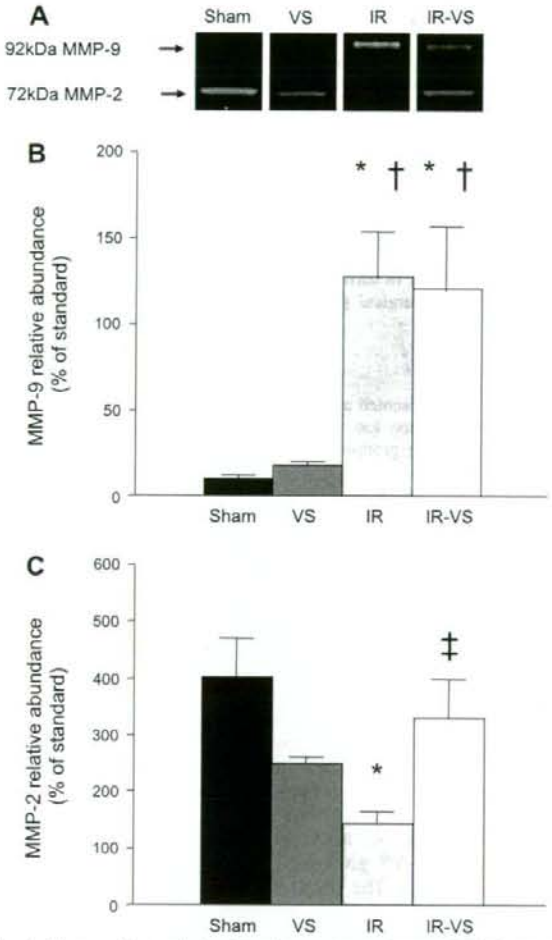


Fig. 1. Zymographic analysis of matrix metalloproteinase (MMP)-9 and -2 proteins in isolated myocardium. Sham, no myocardial ischemia and no vagal stimulation; VS, no myocardial ischemia with vagal stimulation; I/R, myocardial ischemia-reperfusion; I/R-VS, myocardial ischemia-reperfusion with VS. *A*: representative zymogram showing MMP-9 at 92 kDa and MMP-2 at 72 kDa. *B*: densitometric analysis of relative MMP-9 content expressed as percentage of standard. *C*: densitometric analysis of relative MMP-2 content expressed as percentage of standard. Data are means ± SE. $*P < 0.01$ vs. sham; $\dagger P < 0.01$ vs. VS; $\ddagger P < 0.05$ vs. I/R.

significant differences in baseline TIMP-1 concentrations among the three groups. At 150 min, dialysate TIMP-1 concentration was significantly higher in the VNS and ACh groups than in the ACh-Atr group ($P < 0.05$).

Figure 5 depicts representative microscopic findings of LV tissue around the microdialysis probes in the VNS, ACh, and ACh-Atr groups. Hematoxylin-eosin-stained sections demonstrated only a minimum hemorrhage around the dialysis probe (Fig. 5, *A–C*). TIMP-1-positive cardiomyocytes were detected sparsely but in diffuse distribution throughout the myocardium in the VNS group (Fig. 5*D*). TIMP-1-positive cardiomyocytes were detected over a relatively wide area around the dialysis probe in the ACh group (Fig. 5*E*). TIMP-1-positive cardiomyocytes were also detected but localized close to the dialysis probe in the ACh-Atr group (Fig. 5*F*). Immunoreactive signals of TIMP-1 were restricted to the cytoplasm of cardiomyocytes in all the groups (Fig. 5, *G–I*).

Table 3 summarizes the data of systemic hemodynamics and LV function during the cardiac microdialysis study. In the VNS group, HR decreased significantly compared with that in the ACh and ACh-Atr groups at 150 min. In the ACh and ACh-Atr groups, topical perfusion of ACh or ACh with Atr did not affect the systemic hemodynamics and the LV functions. Except for HR, there were no significant differences in other hemodynamic parameters among the three groups.

## DISCUSSION

The major new findings of the present study were as follows. In ischemia-reperfused myocardium, stimulation of the efferent vagal nerve increased TIMP-1 mRNA and protein levels and reduced endogenous active MMP-9 protein. In normal myocardium, VNS or topical perfusion of ACh through a microdialysis probe increased dialysate TIMP-1 protein level. An increase in the dialysate TIMP-1 protein level induced by ACh perfusion was suppressed by coperfusion of Atr.

The robust increase in total MMP-9 levels after reperfusion in this study (Figs. 1*B* and 2*A*) might be mainly due to the

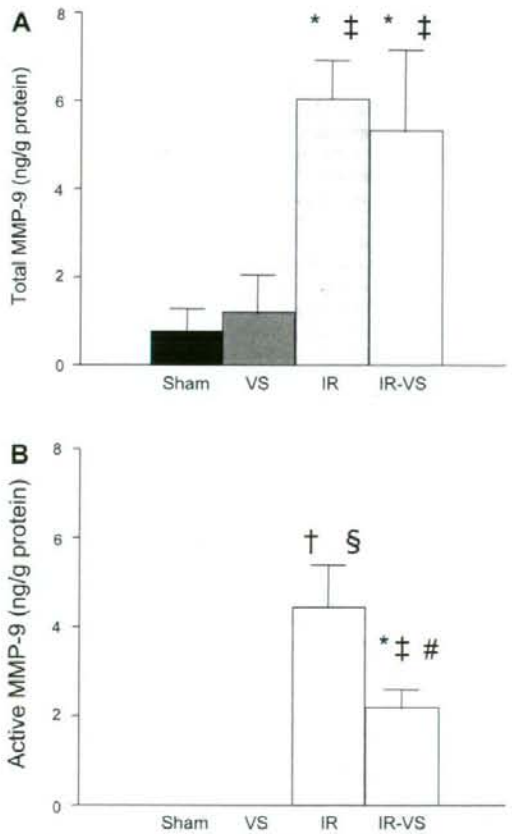


Fig. 2. Bioactivity assay of total (*A*) and active (*B*) MMP-9 protein. $*P < 0.05$; $\dagger P < 0.01$ vs. sham; $\ddagger P < 0.05$; $\S P < 0.01$ vs. VS. $\#P < 0.01$ vs. I/R.

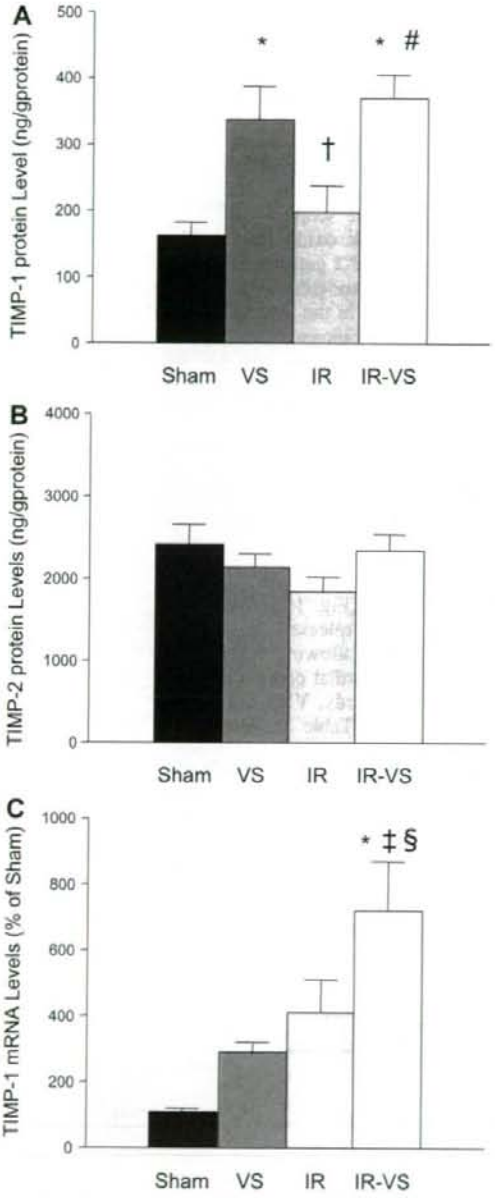


Fig. 3. ELISA measurement of tissue inhibitor of MMP (TIMP)-1 (*A*) and -2 (*B*) protein. Real-time RT-PCR analysis of TIMP-1 mRNA expressed as percentage of sham (*C*). *$P < 0.01$ vs. sham; †$P < 0.05$; ‡$P < 0.01$ vs. VS; §$P < 0.05$; #$P < 0.01$ vs. I/R.

infiltrated neutrophils. Although all cell types, including cardiomyocytes (25, 34) and endothelial cells (41), express MMP-9, neutrophil is an important source of MMP-9 after I/R (26). The level of endogenous active MMP-9 was lower in the I/R-VS group than in the I/R group (Fig. 2*B*). Increased expression of TIMP-1 by VNS (Fig. 3) likely inhibited the conversion of pro-MMP-9 to active MMP-9 and/or inhibited

Table 2. *Hemodynamic parameters during I/R study*

| | Baseline | 60 min | 240 min |
|---|---|---|---|
| HR, beats/min | | | |
| Sham | 317±9 | 334±7 | 326±9 |
| VS | 281±14 | 215±17*‡ | 238±19*‡ |
| I/R | 306±9 | 316±9 | 314±8 |
| I/R-VS | 301±7 | 217±5*‡ | 228±8*‡ |
| MAP, mmHg | | | |
| Sham | 92±3 | 93±4 | 92±3 |
| VS | 98±4 | 91±5 | 89±5 |
| I/R | 102±3 | 95±4 | 88±6 |
| I/R-VS | 99±4 | 88±4 | 83±2 |
| LV $dP/dt_{max}$, mmHg/s | | | |
| Sham | 5,119±263 | 5,308±388 | 4,819±339 |
| VS | 5,040±381 | 3,993±319 | 4,140±302 |
| I/R | 5,524±423 | 5,276±404 | 4,514±467 |
| I/R-VS | 5,672±360 | 4,549±250 | 4,079±188 |
| FS, % | | | |
| Sham | 10.8±0.9 | 10.1±1.0 | 9.3±1.0 |
| VS | 12.2±1.1 | 11.1±1.2 | 10.4±1.6 |
| I/R | 8.7±0.8 | −0.6±0.6*† | 0.1±0.8*† |
| I/R-VS | 8.5±1.3 | −0.6±0.4*† | 1.5±0.7*† |

Values are means ± SE. Sham group, no myocardial ischemia and no vagal stimulation (VS); VS group, no myocardial ischemia with VS; I/R group, myocardial ischemia-reperfusion (I/R); IR-VS, myocardial I/R with VS; HR, heart rate; MAP, mean arterial pressure; LV $dP/dt_{max}$, maximum first derivative of left ventricular (LV) pressure; FS, fractional shortening of anterior wall (risk area). *$P < 0.01$ vs. sham; †$P < 0.01$ vs. VS; ‡$P < 0.01$ vs. I/R.

active MMP-9 itself more potently than in the case without VNS (14). Oxygen free radical induces expression and activation of MMP-9 (17, 41). Reduction of HR by VNS probably reduced myocardial oxygen consumption, ameliorated myocardial ischemia, and reduced oxygen free radicals (30). This may contribute to some extent to the reduction of active MMP-9 in the I/R-VS group.

In the I/R study, TIMP-1 mRNA was significantly higher in the I/R-VS group compared with the sham, VS, and I/R groups (Fig. 3*C*). TIMP-1 mRNA appeared higher in the VS and I/R groups compared with the sham group, although the differences were not significant. Stapel et al. (38) noted increased expression of TIMP-1 mRNA after myocardial I/R in mice. Proinflammatory cytokines such as interleukin-1β induced by

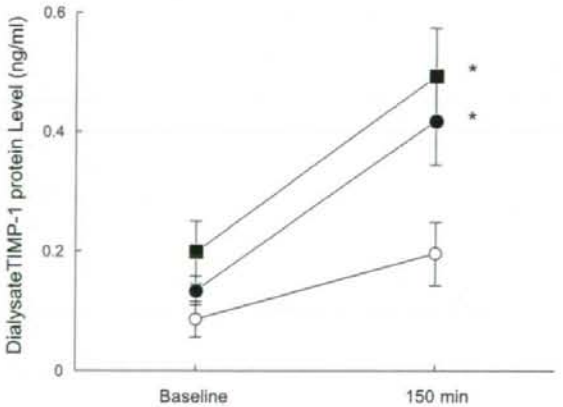


Fig. 4. Dialysate TIMP-1 protein concentration in response to vagal nerve stimulation (■), perfusion of acetylcholine (ACh; ●), or ACh with atropine (Atr) (○). *$P < 0.05$ vs. perfusion of ACh with Atr.